Anaerobic Dehalogenation of Trichloroethene by Encapsulated *Dehalococcoides mccartyi*

by
Eileen Lukens

A THESIS

submitted to

Oregon State University

Honors College

in partial fulfillment of
the requirements for the
degree of

Honors Baccalaureate of Science in Environmental Engineering
(Honors Scholar)

Honors Baccalaureate of Science in Sustainability
(Honors Scholar)

Presented June 3, 2019
Commencement June 2019

AN ABSTRACT OF THE THESIS OF

Eileen Lukens for the degree of Honors Baccalaureate of Science in Environmental Engineering and Honors Baccalaureate of Science in Sustainability presented on June 3, 2019. Title: Anaerobic Dehalogenation of Trichloroethene by Encapsulated *Dehalococcoides mccartyi*

.

Abstract approved: _____

Lewis Semprini

Chlorinated aliphatic hydrocarbons (CAHs) like trichloroethene (TCE) were mostly used to replace drying cleaning fluids which contained hydrocarbons like benzene, and were highly flammable. Through improper disposal, storage, and spills, TCE and its downstream products, like cis-dichloroethene (cDCE) and vinyl chloride (VC), leached into groundwater and threaten human and environmental health. An anaerobic organo-halide respiring bacterium, *Dehalocccoides mccartyi*, can be used to completely dehalogenate TCE to ethene, a non-toxic end-product. *Dehalocccoides mccartyi* uses CAHs as electron acceptors and hydrogen as the electron donor. *Dehalocccoides mccartyi* is a strict anaerobe. Because of this, field tests with anaerobic bacteria must include technologies to protect cultures from oxygen exposure during injection into contaminated wells. Currently, nitrogen blankets are used to protect cultures, but these technologies can be expensive. These challenges could be addressed through anaerobic encapsulation, the process of entrapping cells in a gel matrix to act as a physical barrier between bacteria and the surrounding environment. In addition, encapsulation is an inexpensive technology.

The objective of this study was to determine the methodology for anaerobically encapsulating a culture highly enriched with *Dehalococcoides mccartyi* in sodium alginate gel matrix, compare suspended cell performance with encapsulated cell performance, and determine the effects of oxygen on encapsulated cells. These objectives were achieved by creating an anaerobic 4% wt sodium alginate gel bead solution and combining it with the culture in an anaerobic glove box resulting in a 2% wt sodium alginate – culture solution. Beads were formed by extrusion through a 23G needle into a 0.25% calcium chloride solution. Encapsulated *Dehalococcoides mccartyi* produced TCE dehalogenation rates comparable to suspended culture. However, gel beads deteriorated after two weeks. In addition, rates of TCE dehalogenation decreased after exposure to 0.97% oxygen in the headspace.

Key Words: Bioremediation, Chlorinated Solvents, Encapsulation, Anaerobic, *Dehalococcoides*

Corresponding e-mail address: eil.lukens@gmail.com

Anaerobic Dehalogenation of Trichloroethene by Encapsulated *Dehalococcoides mccartyi*

by
Eileen Lukens

A THESIS

submitted to

Oregon State University

Honors College

in partial fulfillment of
the requirements for the
degree of

Honors Baccalaureate of Science in Environmental Engineering
(Honors Scholar)

Honors Baccalaureate of Science in Sustainability
(Honors Scholar)

Presented June 3, 2019
Commencement June 2019

Honors Baccalaureate of Science in Environmental Engineering and Honors Baccalaureate of Science in Sustainability project of Eileen Lukens presented on June 3, 2019.

APPROVED:

_____

Lewis Semprini, Mentor, representing School of Chemical, Biological, and Environmental Engineering

_____

Tyler Radniecki, Committee Member, representing School of Chemical, Biological, and Environmental Engineering

_____

Mohammad Azizian, Committee Member, representing School of Chemical, Biological, and Environmental Engineering

_____

Toni Doolen, Dean, Oregon State University Honors College

I understand that my project will become part of the permanent collection of Oregon State University, Honors College. My signature below authorizes release of my project to any reader upon request.

_____

Eileen Lukens, Author

Acknowledgements

I would like to thank so many people for supporting me on my journey to completion of this project. First, I would like to acknowledge my undergraduate professors who gave me all the tools I needed to be a successful engineer. I would not be who I am today without them.

I would like to thank Dr. Lewis Semprini for taking me under his wing and supporting me for the past four years. He truly enriched my college experience and not only mentored me in the lab but also helped further my professional and academic career. He always made me feel welcomed and supported. I could not have asked for a better mentor than him. Not to mention he throws great dinner parties.

I would also like to thank Dr. Mohammad Azizian for his mentorship and for being on my committee. Mohammad saved me more times than I can count and knew how to soothe any machine in the lab. He took the time to walk me through procedures and showed me everything I needed to succeed in the lab as well as became a great friend.

I would also like to thank Dr. Tyler Radniecki for his mentorship and for being on my committee. Dr. Radniecki challenged me to push my analysis of a problem to the next level and supported me in my classes along the way.

There are so many graduate student mentors I want to thank who answered my silly questions, were patient with me, and taught me skills in the lab and in life. I especially want to thank Hannah Rolston for being my mentor from day one in the lab and not only teaching me everything I know about how to work in a lab, but also for supporting me in my fellowships and graduate school applications. She is truly an inspiring woman and we need more people like her in the world. I would also like to thank Mitchell Rasmussen, Riley Murnane, and Jon Laurance for countless laughs and Alyssa Saito, Emma Ehret, Marina Cameron, and Krysta Krippaehne for

being empowering women that I aspire to be. I would also like to thank all the other graduate students who came to my aid despite being in different labs like Ashley Berninghaus and Rich Hilliard who lent their knowledge and kindness.

I want to thank my mom, without her I wouldn't be a scientist. She inspires me every day to do my best and to move through the world with confidence. She also supported me every step of the way with late night phone calls and soothing words to alleviate my anxieties.

I would like to thank my undergraduate coworkers who supported me and created a lovely environment to work in like Willow Walker, Allison Burns, and Stephanie Wright. I would especially like to thank my favorite partners in crime, Grant Kresge and Gillian Williams for making me laugh every day. I would also like to extend my gratitude to the countless undergrads in the lab space like Gabi Garza, Elmira Fathe Azam, and others. I would especially like to thank my best friend since sixth grade and lab adjacent partner, Nora Honeycutt, for countless therapy sessions and being my editor while writing our theses. And of course, I would like to thank all my peers outside of the lab who supported me: Manasi Vyas, Sydney Clark, Lauren Roof, Julia Whitaker, and my wonderful partner Cori Elam.

Finally, I want to thank everyone who funded me in my undergraduate career like the those involved in the Sophomore Women Engineering Fellowship, the Johnson Internship Program, the Clean Water Initiative Summer Undergraduate Research Fellowship.

Thank you all!

Table of Contents

List of Figures

List of Tables

Literature Review

History

Chlorinated aliphatic hydrocarbons (CAHs) were mostly used to replace drying cleaning fluids which contained hydrocarbons like benzene, which were highly flammable[1]. Carbon tetrachloride (CT) was one of the first chlorinated solvents to be used in the dry-cleaning industry due to its low flammability[1]. However, it also had applications in floor wax, paints, and essential oil extraction[1]. Usage of CT began to decline when it was discovered that in the presence of moisture and heat, phosgene gas could be produced[1]. Many people were concerned over this because phosgene gas was used as a deadly choking weapon in WWI[2].

In the 1930s, trichloroethene (TCE) and tetrachloroethene (PCE) began to phase out CT due to better recovery methods for those chemicals, but also reduced metal corrosion[1]. PCE was used in dry cleaning and many similar industries as CT[1]. TCE was widely used as it was the most effective cleaning and degreasing agent[1]. Similar to PCE, TCE's high recovery rate, non-flammability, and non-corrosivity made it an ideal candidate for usage in industry[1]. TCE was also used in textiles, general anesthetics, many household cleaning agents, and even in the decaffeination of coffee[1]. Its use continued until 1960 when the environmental movement found its footing in the United States[1].

Chlorinated solvents leached into ground water through leaky storage tanks, accidental spills, and improper waste disposal[3]. Chlorinated solvents can partition between gas and liquid phases following Henry's law[4]. When pure liquid phase of a chlorinated solvent leaks into the subsurface, a dense non-aqueous phase liquid (DNAPL) can form[5]. The formation of DNAPLs are particularly problematic as they act as long-lasting sources of contamination. When water in an aquifer passes through a zone containing a DNAPL, chlorinated solvents dissolve into the passing fluid and can be transported throughout the aquifer. In addition to being distributed as DNAPLs, chlorinated

solvents can also sorb to soils[5]. Sorption is a significant problem in the ground as it traps chlorinated solvents in the solids and aquifer material and makes them difficult to clean[5]. All these various attributes of chlorinated solvents are a concern because they pose risks to human and environmental health. A 1975 study by the National Cancer Institute found that exposure to TCE can cause cancerous tumors to form in mice[6]. In addition, aquifer-fed wetlands are at risk for contamination. A study conducted on four species of North American amphibians found that both PCE and TCE disrupt the development of amphibian embryos[7].

Increased pressure to have strict regulations of industrial chemicals led to the reduced usage of chlorinated solvents. In addition, the 1970 Clean Air Act caused regulation of TCE and PCE emissions due to concerns of ground-level and ozone smog[1]. Trichloroethane (TCA) was introduced to replace TCE, but was eventually banned for similar reasons[1]. Furthermore, the dumping of toxic wastes was banned in 1976 under the Resource Conservation and Recovery Act[8]. Eventually, in 1980 the Comprehensive Environmental Response, Compensation, and Liability Act (CERLA) was passed by Congress in response to public concern from toxic waste incidents such as Love Canal, New York[8]. CERLA was the first nationwide emergency response program of its kind providing toxic waste information and enforcing hazardous waste clean up[8]. Within CERLA, a trust fund (often referred to as Superfund) was created in order to support the clean-up of toxic waste. Following that in 1983, the EPA created the National Priority List (NPL) which specified 406 sites of concern to be cleaned up under the Superfund[1]. TCA, PCE, TCE, and CT were the four most common contaminants found at the Superfund sites[1].

Treatment Options

Several methods of treatment for groundwater contamination exist including chemical, thermal, physical, and biological treatment. Chemical treatment options include oxidation and reduction[1]. In-situ chemical oxidation has the advantage of rapid treatment[8]. In addition, the proper

oxidant can treat a variety of chemicals[9]. Furthermore, the end products of in-situ chemical oxidation are generally innocuous[9]. However, chemical oxidation can also mobilize metals in the groundwater[9]. The oxidant can be consumed by other materials in the aquifer as well as the target materials[9]. Furthermore, in-situ chemical oxidation is not ideal for groundwater with dilute and low concentrations of contaminants[9]. Thermal treatment options include electric resistive heating, thermal conductive heating, and hot fluid injection[1]. Thermal treatment can quickly and reliably clean up chlorinated solvents; however, the act of heating the soils damages their natural properties[10]. In addition, there has been little work to improve this technology despite its success[10]. Physical treatment includes air stripping, activated carbon, bioventing, and soil vapor extraction[1]. In soil vapor extraction, clean air is pumped into contaminated soil areas and then the contaminated air is pulled out with vacuums[11]. Pump and treat is another common method of cleanup. In this system, contaminated water is pumped to the surface and then treated with air stripping or another technology[12]. Air stripping is effective for highly volatile compounds but must be used in conjunction with another technology in order to transform the contaminant into a non-toxic product[13]. Biological treatment methods, often referred to as bioremediation, utilize microorganisms to clean groundwater[1]. Bioremediation is advantageous in that some native microbes to the aquifer can be stimulated to degrade chlorinated compounds without the need for bioaugmentation[14]. However, bioremediation is a much slower process than other treatment options and has limited success in high concentrations of contaminants as these conditions can be toxic to microorganisms[13]. Bioremediation will be the focus of this review.

Bioaugmentation

Bioaugmentation is one form of bioremediation and is the process of introducing non-native microbes into the subsurface in order facilitate desired microbial reactions. Bioaugmentation is

advantageous for several reasons. For one, bioaugmentation reduces the time frame for remediation compared to biostimulation[1]. Biostimulation is the process which remediates contaminated sites by enhancing aquifer conditions for native microbial populations[15,16]. In addition, bioaugmentation can be useful when native dechlorinating species are present at low concentrations or when biostimulation is unsuccessful if the microorganisms are well adapted to degrading compounds of interest[1]. Bioaugmentation has been successful in field-scale tests as well as at wastewater treatment plants[17,18].

Microorganisms can respire chlorinated solvents both aerobically and anaerobically. The metabolism of microorganisms allows certain species to degrade chlorinated solvents. Aerobic cometabolism is the process by which a microbe, in the presence of certain substrates, will produce unique enzymes that degrade chlorinated solvents. In the case of aerobic cometabolism, VC and cDCE can serve as electron donors[19,20]. Another type of respiration is the anaerobic reductive dehalogenation pathway with hydrogen as the electron donor[21]. In this case, chlorinated solvents act as the electron acceptors. Anaerobic respirators have an advantage over aerobes in that they can transform chlorinated solvents at higher concentrations making them effective for DNAPL clean up[1]. This second type of respiration will be the focus of this review.

Anaerobic reductive dehalogenation can be performed by a variety of organo-halide respiring bacteria (OHRB)[22]. There are various species of OHRB including *Desulfitobacterium*, *Geobacter*, and *Dehalococcoides mccartyi*[22]. *Dehalococcoides* have various reductive dehalogenation proteins (rdhA) responsible for the de-chlorination of solvents[22]. PceA dechlorinates PCE to TCE. TceA dechlorinates TCE to ethene and VcrA dechlorinates TCE, DCE, and VC to ethene[22] (Figure 1). However, *Dehalococcoides mccartyi* more efficiently dechlorinates TCE when other electron

acceptors like DCE and VC are present, making competition with other OHRB key to the success of *Dehalococcoides*[23].

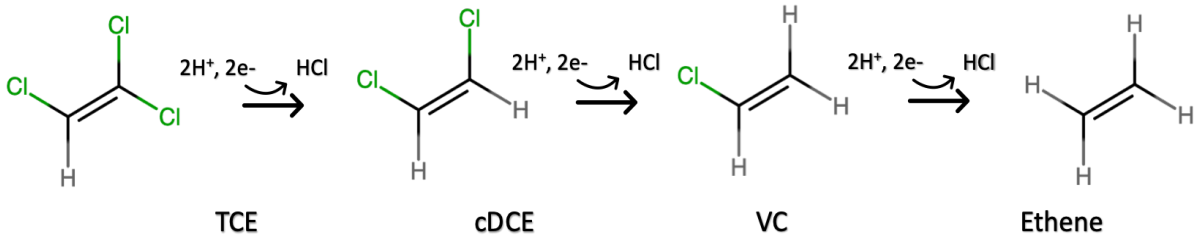

Figure 1: Reductive dehalogenation of TCE. Hydrogen acts as the electron donor and replaces the chlorines. The chlorinated solvents act as electron acceptors and chlorines become an acid in solution.

Anaerobic bacteria lack certain enzymes that protect them from damaging oxygen reduction products[24]. Reduction products such as the superoxide anion and free hydroxyl radical are damaging to the cells[24]. Aerobic and facultative microbes compensate for these harmful products with the production of an enzyme called superoxide dismutase[24]. Anaerobic cells like *Dehalococcoides mccartyi* do not have this protective enzyme and are therefore harmed in the presence of oxygen. This inhibits the ability of *Dehalococcoides mccartyi* to perform reductive dehalogenation, particularly the dechlorination of vinyl chloride to ethene[25].

Common practice for keeping *Dehalococcoides mccartyi* protected from oxygen exposure during field implementation includes transporting the culture in a steel carrying vessel under a nitrogen blanket (Figure 2)[26,18]. A pilot test to transform PCE to ethene at the Kelly Air Force Base near San Antonio, Texas was conducted with a bacterial consortium containing phylogenetic relatives to *Dehalococcoides ethenogenes*[26]. The culture was transported to the site under a N_2/CO_2 atmosphere in 8-L stainless steel vessels[26]. Furthermore, to reduce the amount of oxygen at the site, the water column and air in the well was sparged with argon before the culture was introduced to the well with an argon-flushed delivery line[26].

Figure 2: KB-1 is a dehalococcoides culture distributed by sirem-lab. Transport of the material occurs under a nitrogen blanket. Photo Source: www.siremlab.com

Encapsulation

Cell immobilization has been investigated for medical applications[27]. However, environmental applications are just emerging. One form of cell immobilization is gel encapsulation which has minimal loss of cell viability[28]. These gel matrices can be made of natural or synthetic polymers and are usually formed into small 1-5 mm diameter beads[28]. Generally, polymers are selected based on the desired gel properties such as mechanical strength, porosity, and hydrophobicity[28]. However, cell growth inside the polymers can degrade the mechanical strength of the matrix and cause the matrix to deteriorate[28]. Encapsulation can be performed with a variety of polymers such as alginate, cellulose, gellen gum, and others[28]. Interestingly, alginate is derived from brown algae and can gel by cross-linking with calcium[27] (Figure 3). However, ionically cross-linking can be unstable due to the mobility of divalent cations which can attach to other compounds in media solutions[27].

Immobilization is of interest for *Dehalococcoides mccartyi* because it may protect the culture from oxygen and lead to better dispersion throughout aquifers in field applications.

Clogging of aquifers can occur in in-situ bioremediation due to the excessive growth of bacteria near the injection site[29]. Encapsulated cells may reduce this effect. In a column packed with sand, gellen gum microbeads were found to distribute evenly throughout the column[30]. In addition, encapsulation may provide a physical barrier between the cells and the environment potentially allowing time for the cells to acclimate to new conditions[31]. Immobilization can essentially create micro-environments for the cells inside the more hostile macro-environment of an aquifer[32]. Gel matrices could potentially control diffusion rates of contaminants to the cell which is of interest to *Dehalococcoides mccartyi* with regards to oxygen.

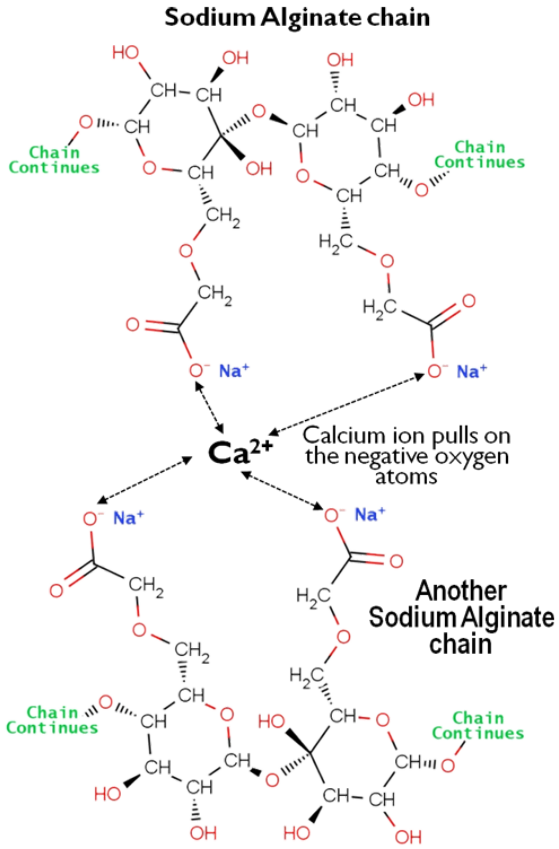

Figure 3: The crosslinking of sodium alginate with calcium (Ca2+). Image source: www.chemistryland.com

Objectives

This project aimed to address several key objectives including…

- Determining the methodology for anaerobically encapsulating a culture highly enriched with *Dehalococcoides mccartyi* in sodium alginate gel matrix
- Comparing suspended cell performance to encapsulated cell performance
- Determining if encapsulation will protect cells from oxygen exposure

Materials and Methods

Dehalococcoides mccartyi was encapsulated by creating an anaerobic 4% wt sodium alginate solution and combining with an equivalent volume of culture to create a 2% wt sodium alginate-culture solution. Encapsulated cells were then exposed to TCE to compare rates of degradation with non-encapsulated cells in solution (suspended cells). A flow chart of the encapsulation procedure can be found in Figure 4. Table describing materials and solutions used can be found in Table 3, Appendix B.

Victoria-Stanford 2L Culture

The dehalogenating culture used in this study was the Victoria-Stanford consortium. The Victoria-Stanford 2L (VS2L) culture originated from a PCE-contaminated site in Victoria, Texas[33]. Native *Dehalococcoides* were identified as one of the dechlorinating species at this site[34]. In the Semprini laboratory, *Dehalococcoides* and other OHRB in the VS2L culture have been developed into a robust population in a continuous stir tank reactor (CSTR). Due to the slow growth of this culture, the mean hydraulic residence time of the CSTR is 50 days[23] (Figure 5). The CSTR receives a continuous feed of saturated TCE to its solubility limit in water. Prior to this encapsulation experiment, the VS2L culture was fed formate excess (45mM), deficit (25mM), and finally formate excess again[23]. Excess formate allows for the production of hydrogen to complete dechlorination and also acts as a buffering mechanism to prevent changes in pH during dechlorination[35]. Furthermore, the culture was effective at stably transforming TCE to ethene[23].

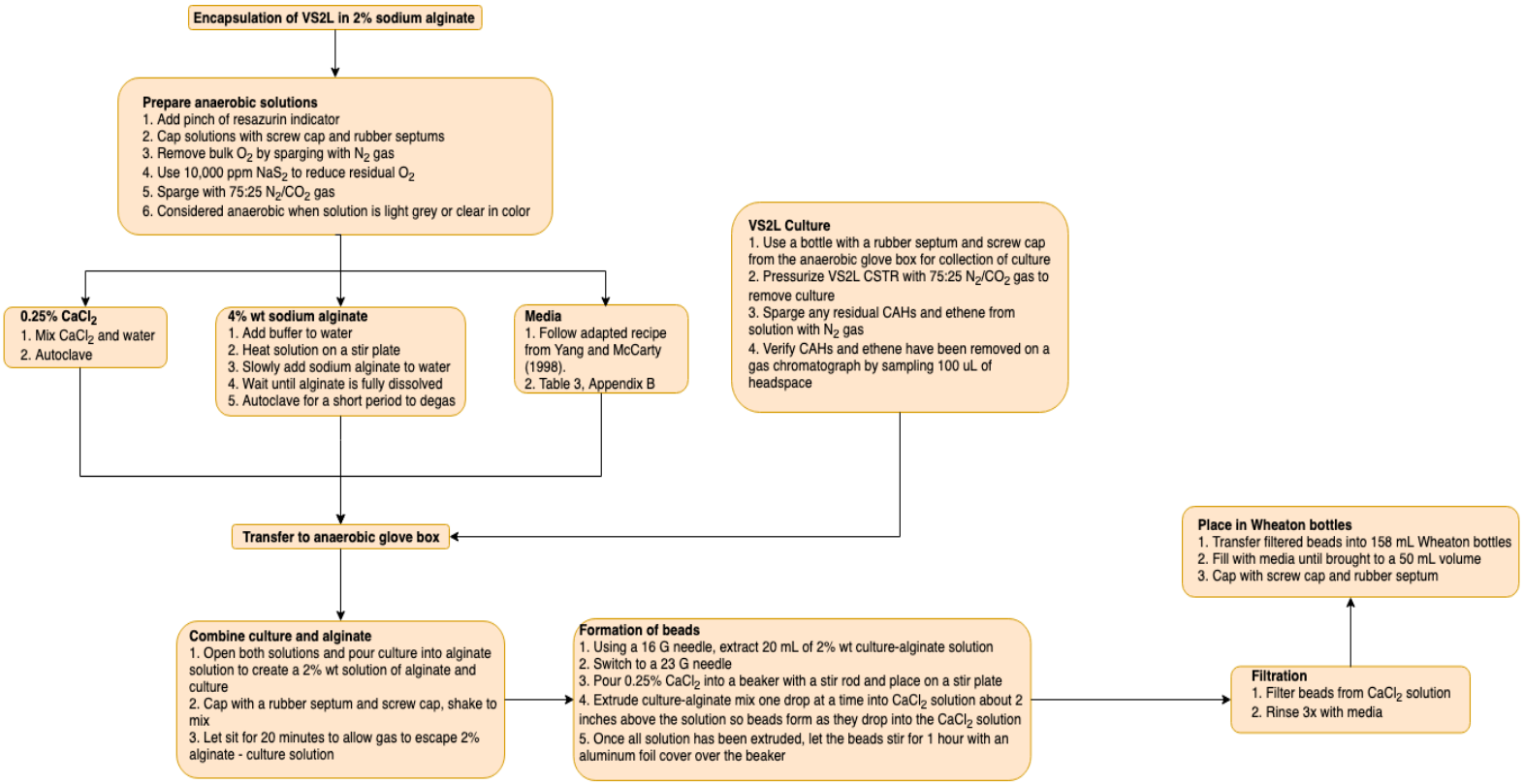

Figure 4: Flow chart of encapsulation procedure

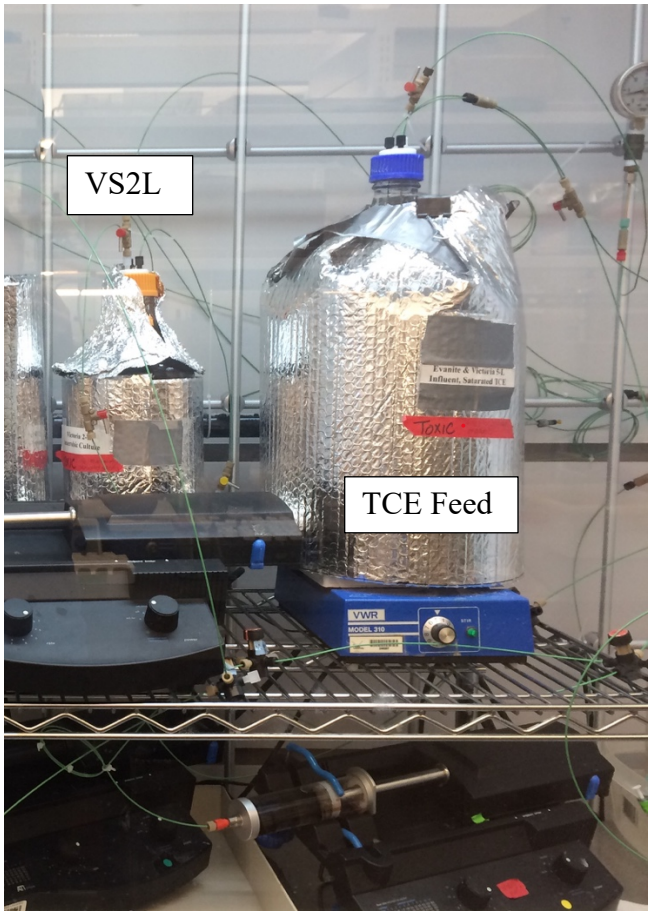

Figure 5: VS2L CSTR (left) containing mixed Dehalococcoides. Reactor fed by saturated TCE and 45mM formate (right). Retention time of 50 days.

Creating Anaerobic 4% Alginate Solution

The alginate solution was based on studies conducted by Mitchell Rasmussen and Paige Molzahn[36,37]. In a laminar flow hood, 60 mL of deionized water and 1 mL of solution 2 were added to a 250 mL borosilicate Wheaton bottle with a screw cap. The solution was heated and stirred on a stir plate. In small increments, 2.4 g of sodium alginate was added to the mixture to create a 4% sodium alginate solution. The mixture was very viscous and dissolved slowly. The pH was checked with a paper pH strip to ensure a pH of 7. The sodium alginate was then autoclaved for 5-10 minutes to sterilize the mixture. The alginate was left to cool to room temperature. The 4% sodium alginate was transferred to an autoclaved 250 mL borosilicate glass Wheaton bottle with a screw cap, rubber septum, and stir bar. Before capping, a small pinch of resazurin was added to the bottle

to act as an oxygen indicator. The bottle was then placed in an up-flow hood with a stir plate. As the solution was mixed, the 4% alginate was sparged with nitrogen gas to remove oxygen. After 20 minutes, 0.3 mL of 15,000 ppm sodium sulfide was added as a reductant to the bottle through the rubber septum and bubbled for another 20 minutes with purified 75:25 N_2/CO_2 gas. Process was considered complete when gel transitioned from dark blue to pink to a semi-clear grey which indicated oxygen was not present and anaerobic conditions were achieved (Figure 6).

Figure 6: 4% wt sodium alginate gel transitioning from blue to pink to grey. Bottle capped with screw cap and rubber septum.

Culture Collection

158 mL borosilicate bottles were retrieved from the anaerobic glove box. The gas headspace of the VS2L culture was checked using a gas chromatograph to ensure that complete transformation of TCE to ethene was occurring inside the CSTR. A tube furnace was heated to 600°C where 75:25 N_2/CO_2 gas was purified and used to pressurize the VS2L culture. Liquid sample lines were cleared of oxygen by running culture through the lines and collecting the liquid in a waste container. Liquid samples were then collected into 158 mL Wheaton bottles with rubber

septums and screw caps. As sample was collected, a gas needle was placed into the rubber septum to release pressure. Once the desired culture volume had been obtained (180 mL), CSTR was returned to normal function and sample lines were closed. Culture that had been collected was then purged with N_2 gas for 20 minutes to remove residual gases and CAHs. Removal of CAHs was verified on a gas chromatograph.

Creating Anaerobic $CaCl_2$ Solution

Two solutions of approximately 400 mL of 0.25% $CaCl_2$ were autoclaved in 500 mL Wheaton bottles with a rubber septums and stir bars. After the solutions cooled, a pinch of resazurin was added as an oxygen indicator. The solutions were bubbled and stirred for 15 minutes with N_2 gas. The solutions were then bubbled with 75:25 N_2/CO_2 gas and 0.1 mL of 15,000 ppm sodium sulfide was added until the solution turned clear in color.

Suspended Cells

Suspended cell bottles were created by combining 10 mL of culture with 40 mL of anaerobic media in a 158 mL Wheaton bottle inside the anaerobic glove box. Suspended cell bottles were brought into the glove box to expose the cells to the same conditions the encapsulated cells would experience. The bottles were then capped with rubber septums and sealed with parafilm. Cell masses in each bottle were determined from a total suspended solids analysis of the VS2L CSTR to get cell concentrations. Then the total mass of cells inside each bottle was determined from the volume of cells added to each bottle multiplied by the VS2L CSTR cell concentration. The total cell mass inside each bottle was 0.46 mg.

Encapsulating Anaerobic Cells

The 4% wt alginate solution was combined with an equivalent volume of culture to create a 2% wt alginate and cell solution inside the anaerobic glove box. The result was an equivalent cell mass as in the suspended bottles of 0.46 mg. The bottle was capped with a screw cap and

rubber septum. The culture was shaken to mix and set aside to allow gas bubbles to exit the solution. Gel beads were created by doing the following procedure. Using a 16G needle, 20 mL of alginate and cell solution was collected into a 20 mL plastic syringe. The needle on the syringe was then switched to a 23G needle. On a stir plate, 130 mL of 0.25% anaerobic $CaCl_2$ solution was stirred in a beaker as alginate cell solution was slowly added one drop at a time into the $CaCl_2$ solution for cross-linking (Figure 7). The forming alginate-cell beads were allowed to cross-link for 15 minutes or 1 hour. The longer time was to create more strongly cross-linked beads. Beads were gravity filtered and washed three times with anaerobic media to ensure the removal of $CaCl_2$ solution. Each bead was estimated to have had 3.25 x 10^-4 mg cells (Equation 5). Beads were then placed into 158 mL Wheaton bottles. Bottles were brought to 50 mL volume with anaerobic media and capped with a screw top and rubber septum. Once bottles were removed from the anaerobic glove box, caps were sealed with parafilm.

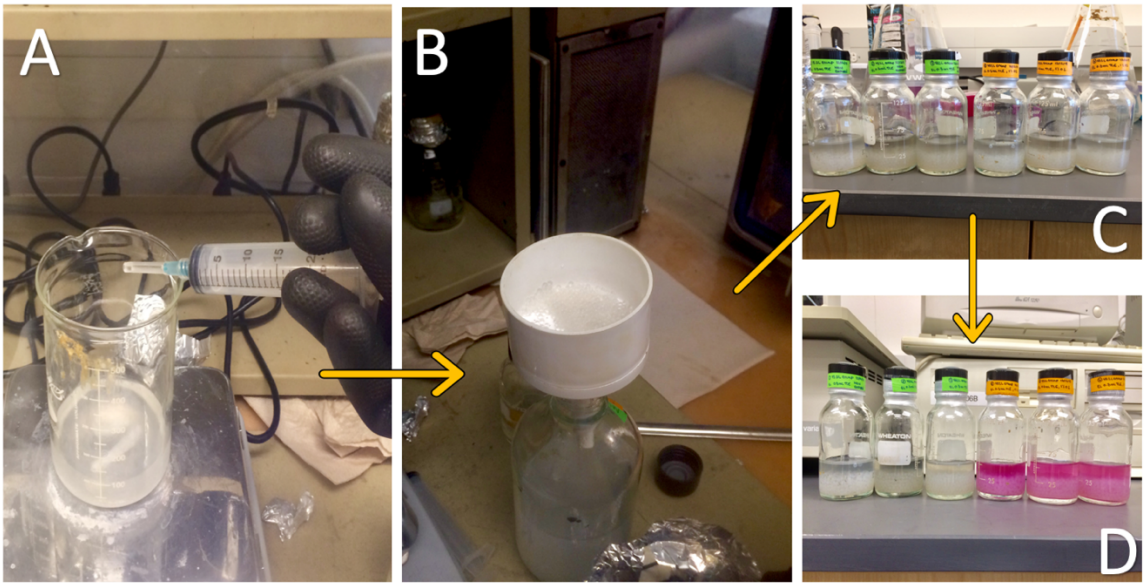

Figure 7: (A) 20 mL 2% sodium alginate with culture extruded through a 23G needle into a 0.25% $CaCl_2$ bath where the beads cured for 1 hour. (B) Beads gravity filtered from $CaCl_2$ solution and washed three times with anaerobic media. (C) Beads placed in 158 mL glass Wheaton Bottles and brought to 50 mL with anaerobic media. Sealed with parafilm. (D) 5 mL air added to the headspace of half the bottles. Pink color from resazurin indicator in media and beads.

Oxygen Exposure

All bottles contained a headspace of 108 mL. For both encapsulated bottles and suspended bottles, a 5 mL vacuum was pulled under an up-flow hood using a 5 mL plastic syringe. 5 mL of air was added to half the bottles so three bottles had a headspace with 0.97% oxygen (Equation 4). Bottles were shaken until solution turned pink from the reaction of oxygen with resazurin (Figure 7).

Experimental Start and Maintenance

All bottles were given 0.3 mL of TCE from the CSTR feed which contained saturated TCE to its solubility limit in water and excess formate (45 mM). This resulted in an initial liquid concentration of 32.4 μM TCE. Bottles were shaken vigorously and immediately measured on the gas chromatograph flame ionization detector to obtain initial measurements. This was considered the experimental start time. Degradation of TCE was monitored approximately every 20 minutes. In between sampling periods, bottles were stored in a 25°C dark room on a 200 rpm shaker table.

Analytical Methods

Gas Chromatography

TCE, cDCE, VC and ethene were measured on a Hewlet-Packard 6890 gas chromatograph with a flame ionization detector. The gas chromatograph contained an Agilent 115-3432 GSQ capillary column (30m x 530 μm x 0.00 μm normalized) with a max temperature of 250°C and 15 mL/min gas flowrate. TCE, cDCE, VC and ethene had retention times of 5.4, 2.7, 0.8, and 0.6 minutes respectively. By comparing peak areas produced by the analysis to standard curves, concentrations of contaminants in the gas phase were determined (Figures 76, 77, 78, 79, Appendix A). Then, using Henry's law and the volume of the gas and liquid compartments, the total mass of

contaminant was determined (Table 1 Appendix B; Equations 1, 2 Appendix C). For encapsulated cells, contaminants were assumed to not sorb onto the sodium alginate gel matrix.

Rate Modeling

Rates were determined using a linearization method as well as through an adapted sum of least squared errors modeling method. For the converted linear method, rates of transformation were determined by adding together all the masses of downstream chlorinated compounds of the compound of interest at each time point (Equation 3). Then a linear regression was fit to the data. For example, TCE transformation was determined from the addition of the masses of ethene, VC, and cDCE formed. Linearized rates were considered a good fit to the data if the R-squared values were greater than 0.98.

The non-linear sum of least squared errors method (referred to as "km" in the charts) uses weighted least-squares analysis to find the best-fit values from the integrated Monod equation[38]. In general, this method produces more reliable results than linearized methods[38]. For this study, the non-linear sum of least squared errors method was adapted to include the inhibition between chlorinated ethenes[39]. The model includes the inhibitory effects of TCE on cDCE and VC dechlorination as well as the effects of cDCE on VC dechlorination to ethene [39]. Because of this, the non-linear sum of least square errors model generally predicts higher degradation rates than the converted linear rates.

Results and Discussion

Four sets of experiments were performed (Figure 8). In each set for each cell condition, suspended or encapsulated, triplicate bottles were made. Three sets compared suspended cell performance versus encapsulated cell performance. Performance was judged based on the rates of degradation of chlorinated ethenes. Sets 1 and 2 saw multiple additions of TCE. Set 4 demonstrated the effects of oxygen on suspended and encapsulated cells.

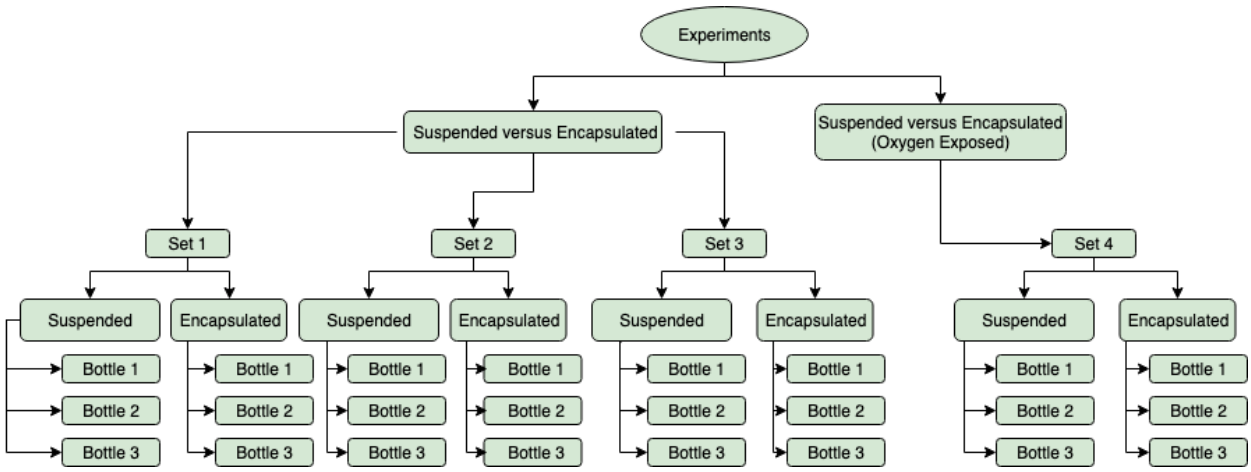

Figure 8: Experimental matrix

Set 1 – Suspended VS Encapsulated

The first set of suspended versus encapsulated cells showed successful encapsulation of *Dehalococcoides mccartyi.* Beads were spherical and 2-3 mm in diameter. Beads were non-uniform due to being formed by hand and not mechanically (Figure 9).

Figure 9: Size of biotic beads shown against a VWR ruler for scale. Beads were 2-3 mm in diameter. Pink color is a result from resazurin indicator reacting with oxygen in the surrounding environment.

Set 1 bottles were spiked with a liquid concentration of 32.4 µM TCE at the start of the experiment. Converted linear rates were found from the accumulation of downstream products

(Figures 10, 11). Converted linear rates did not account for the effects of inhibition between chlorinated compounds. Modeled rates (km) did account for effects of inhibition between chlorinated ethenes and therefore resulted in higher rates of chlorinated ethene degradation (Figures 12, 13). Higher rates of degradation were seen for sets 1-3 for modeled (km) rates. For set 1, modeled (km) degradation rates for TCE and VC fell within 1 standard deviation of each other for suspended cells and encapsulated cells (Figures 14, 15). DCE degradation rates fell within 2 standard deviations. This indicates that the mixed *Dehalococcoides* culture is resilient when encapsulated. Rates of degradation are proportional to those produced by Ehret (2018)[40].

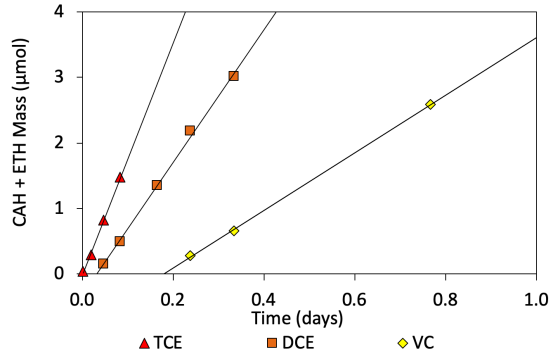

Figure 10: Converted linear rates of degradation of chlorinated ethenes for suspended cells in set 1. Data points represent experimental data from bottle 1. Black lines represent linear trends. Set 1 suspended cells were done in triplicate. Figures 44 and 48 show the other two bottles for suspended cells.

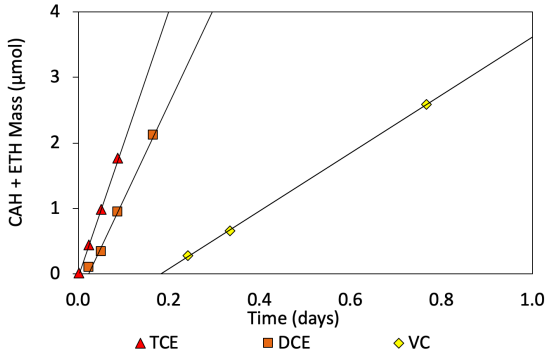

Figure 11: Converted linear rates of degradation of chlorinated ethenes for encapsulated cells in set 1. Data points represent experimental data from bottle 1. Black lines represent linear trends. Set 1 encapsulated cells were done in triplicate. Figures 45 and 49 show the other two bottles for encapsulated cells.

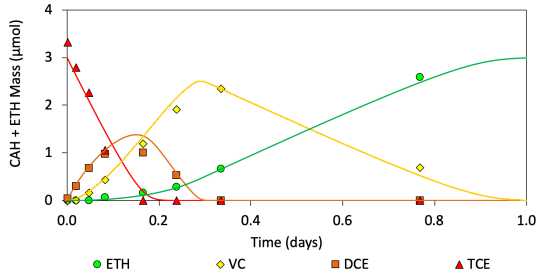

Figure 12: Model (km) rates of degradation of chlorinated ethenes for suspended cells in set 1. Data points represent experimental data from bottle 1. Solid lines represent model prediction. Set 1 suspended cells were done in triplicate. Figures 46 and 50 show the other two bottles for modeled suspended cells.

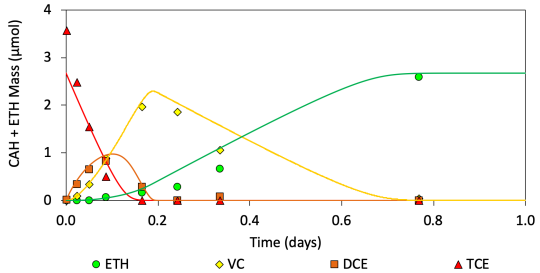

Figure 13: Model (km) rates of degradation of chlorinated ethenes for encapsulated cells in set 1. Data points represent experimental data from bottle 1. Solid lines represent model prediction. Set 1 encapsulated cells were done in triplicate. Figures 47 and 51 show the other two bottles for modeled encapsulated cells.

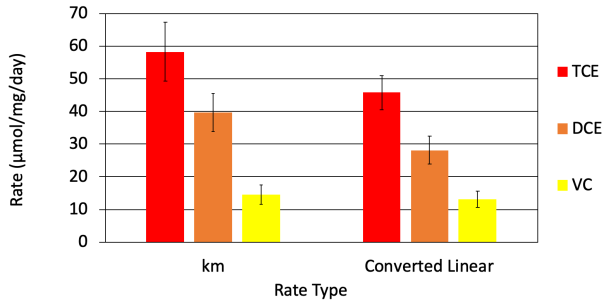

Figure 14: Rates of chlorinated ethene degradation for set 1 suspended cells. Bars represent an average of three trials. Error bars represent standard deviation between three trials. km represents non-linear sum of least squared errors model which accounts for inhibition while converted linear rates do not.

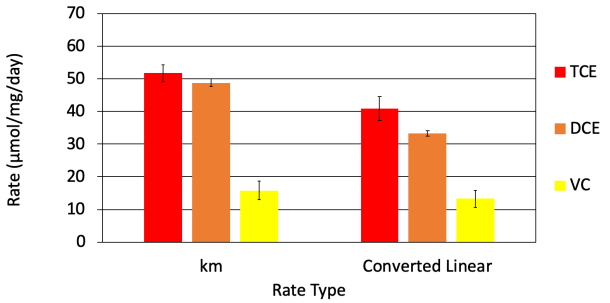

Figure 15: Rates of chlorinated ethene degradation for set 1 encapsulated cells. Bars represent an average of three trials. Error bars represent standard deviation between three trials. km represents non-linear sum of least squared errors model which accounts for inhibition while converted linear rates do not.

Beads appeared to deteriorate after two weeks in solution on the shaker table at 200 rpm. This was indicated by the cloudiness of the media solution (Figure 16). Suspended cell bottles of the same age were not cloudy in appearance suggesting the presence of alginate was the cause of the cloudiness and not cell growth. Beads may have deteriorated for several reasons. Calcium is the cross-linking cation and may have been pulled from the gel matrix into solution due to the constituents that make up the anaerobic media (Table 2, Appendix B). Media constituents include sodium, phosphate, and magnesium. Literature suggests that constituents like these can contribute to gel deterioration[28]. In addition, it is unknown whether *Dehalococcoides mccartyi* or other bacteria in the mixed culture may be able to use alginate as a substrate.

Figure 16: Photo of suspended and encapsulated cells for set 1 on the 3rd day of the experiment (left). Photo of the encapsulated cells 9 days after start of experiment (right). Media that encapsulated cells were suspended in appeared cloudy suggesting the alginate beads were deteriorating.

In an abiotic encapsulated bottle suspended in media and TCE, beads seemed to hold together better than those encapsulated with microbes but still experienced some degradation (Figure 17). Degradation of TCE occurred in this bottle but much slower due to the media properties for abiotic degradation of CAHs. Bead condition also degraded but much slower than biotic beads. In an abiotic encapsulated bottle suspended in deionized water (DI) and TCE, beads also seemed to hold together longer than biotic beads (Figure 18). Although only one trial was done, abiotic beads suspended in DI appeared to hold up only slightly better than abiotic beads suspended in media. Regardless, the presence of microorganisms seemed to have played a key role in the longevity of the beads. Interestingly, very little cell growth occurred per injection of TCE suggesting that perhaps a different microbially mediated process contributed to the degradation of the beads such as consumption of alginate as a substrate (Equation 6).

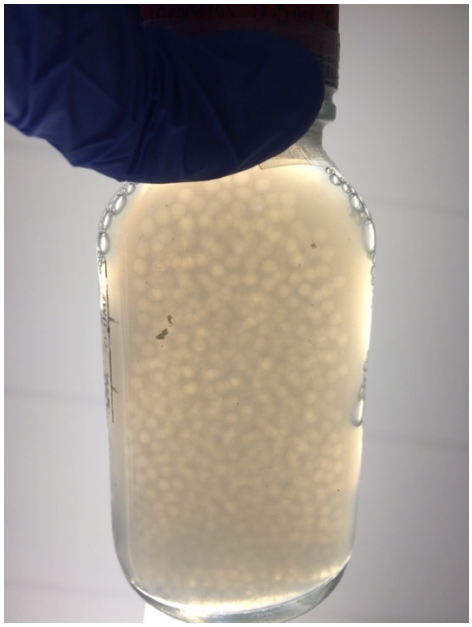

Figure 17: Deteriorated condition of abiotic beads suspended in media solution made August 21st, 2018. Photo taken April 1st, 2019.

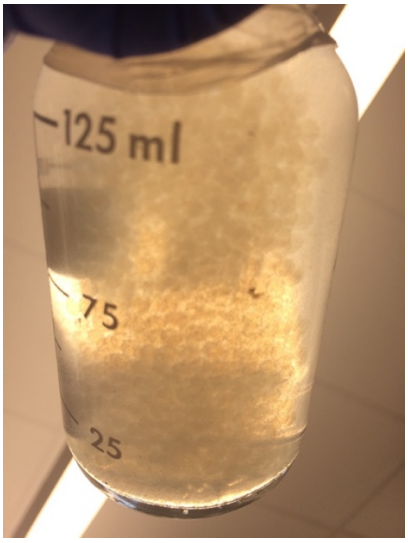

Figure 18: Condition of abiotic beads suspended in DI solution made September 6th, 2018. Photo taken April 1st, 2019. Some degradation of beads over the 7-month period.

Set 2 – Suspended VS Encapsulated

Figure 19: Set 2 suspended (left) and encapsulated (right) cells on day 1 of experiment.

Set 2 resulted in encapsulated beads similar to those seen in Set 1 (Figure 19). Set 2 beads were also 2-3 mm in diameter and spherical in shape (Figure 20). For set 2, encapsulated cells were cured for 1 hour instead of 15 minutes in order to address stability issues with the bead. No difference in the longevity of the beads was seen between set 1 and set 2.

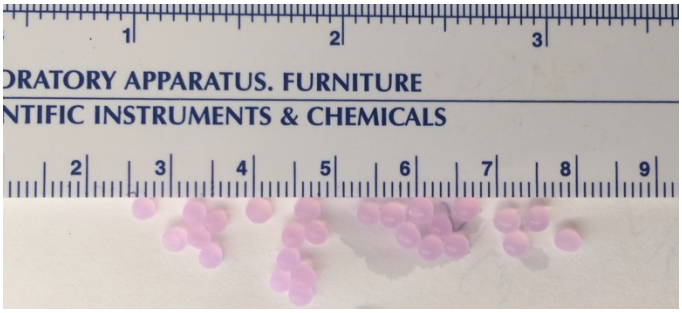

Figure 20: Size of biotic beads shown against a VWR ruler for scale. Beads were 2-3 mm in diameter. Pink color is a result from resazurin indicator reacting with oxygen in the surrounding environment.

Despite collecting the cells on the same day, the second set (set 2) of suspended and encapsulated cells performed very differently (Figures 21, 22, 23, 24, 25, 26). Suspended cells were not taken into the anaerobic glove box with the encapsulated cells. About halfway through the experiment, the suspended cells turned pink indicating exposure to oxygen hence the lower rates seen. Set 2 encapsulated cells performed well with slightly lower rates of degradation than set 1 likely due to cell collection for sets 1 and 2 occurring on different days (Figure 26).

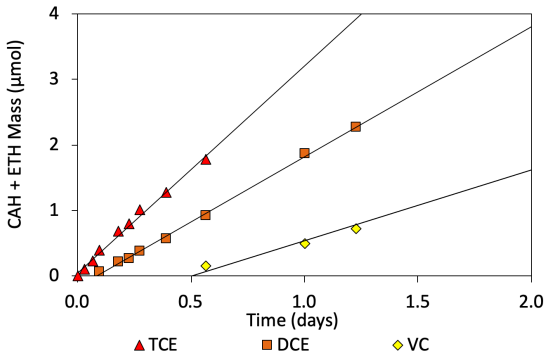

Figure 21: Converted linear rates of degradation of chlorinated ethenes for suspended cells in set 2. Data points represent experimental data from bottle 1. Black lines represent linear trends. Set 2 suspended cells were done in triplicate. Figures 52 and 56 show the other two bottles for suspended cells.

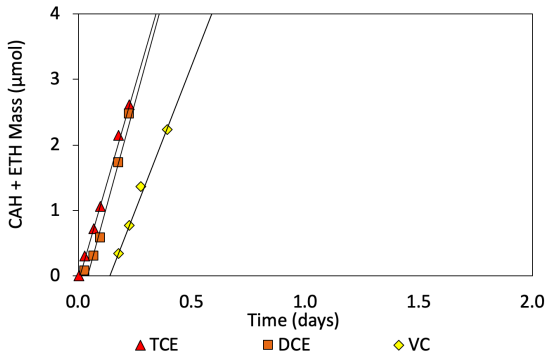

Figure 22: Converted linear rates of degradation of chlorinated ethenes for encapsulated cells in set 2. Data points represent experimental data from bottle 1. Black lines represent linear trends. Set 2 encapsulated cells were done in triplicate. Figures 53 and 57 show the other two bottles for encapsulated cells.

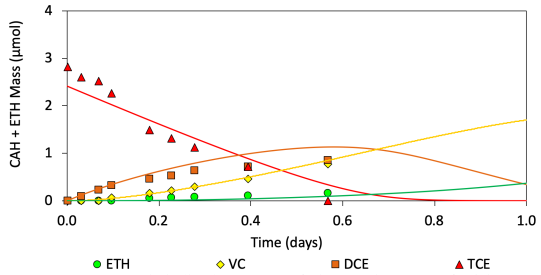

Figure 23: Model (km) rates of degradation of chlorinated ethenes for suspended cells in set 2. Data points represent experimental data from bottle 1. Solid lines represent model prediction. Set 2 suspended cells were done in triplicate. Figures 54 and 58 show the other two bottles for modeled suspended cells.

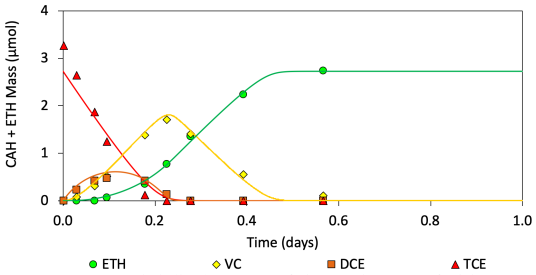

Figure 24: Model (km) rates of degradation of chlorinated ethenes for encapsulated cells in set 2. Data points represent experimental data from bottle 1. Solid lines represent model prediction. Set 2 encapsulated cells were done in triplicate. Figures 55 and 59 show the other two bottles for modeled encapsulated cells.

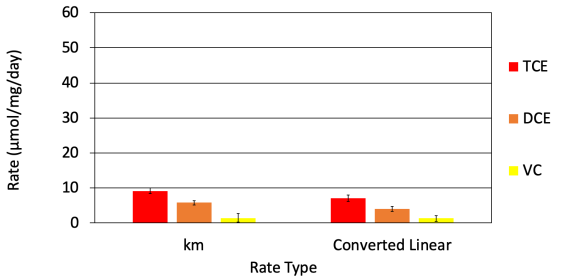

Figure 25: Rates of chlorinated ethene degradation for set 2 suspended cells. Bars represent an average of three trials. Error bars represent standard deviation between three trials. km represents non-linear sum of least squared errors model which accounts for inhibition while converted linear rates do not.

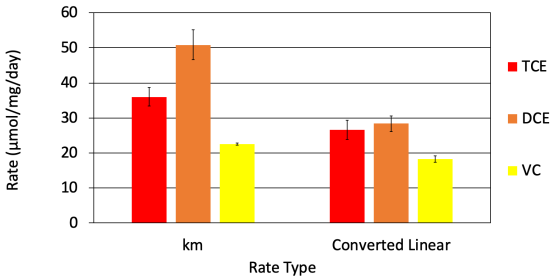

Figure 26: Rates of chlorinated ethene degradation for set 2 encapsulated cells. Bars represent an average of three trials. Error bars represent standard deviation between three trials. km represents non-linear sum of least squared errors model which accounts for inhibition while converted linear rates do not.

Set 3 – Suspended VS Encapsulated

The third set (set 3) of suspended cells and encapsulated cells performed similarly to each other (Figures 27, 28, 29, 30, 31, 32). Although cells for suspended and encapsulated reactors were collected on different days from the VS2L CSTR, cells were treated the same and suspended cells were exposed to the glove box environment. Rates of chlorinated ethene degradation in set 3 were slightly lower than those seen in set 1 which is likely due to the cells being collected on different days from the VS2L CSTR. Although dechlorination time for encapsulated cells appear longer than suspended cells, the rates are actually very similar as seen by the converted linear and non-linear modeled rates (Figures 31, 32). This is because 5x the cell mass was accidentally added to

the suspended cells. When looking at the converted linear and model rates based on cell mass, the rates are actually very similar. Modeled rates for suspended and encapsulated cells for TCE and DCE degradation were within 1 standard deviation of each other. Modeled VC rates of degradation for suspended and encapsulated cells fell within three standard deviations of each other.

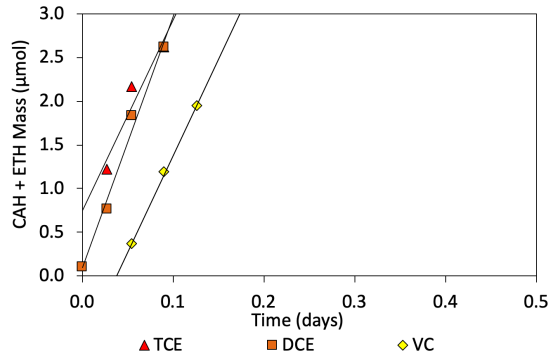

Figure 27: Converted linear rates of degradation of chlorinated ethenes for suspended cells in set 3. Data points represent experimental data from bottle 1. Black lines represent linear trends. Set 3 suspended cells were done in triplicate. Figures 60 and 64 show the other two bottles for suspended cells.

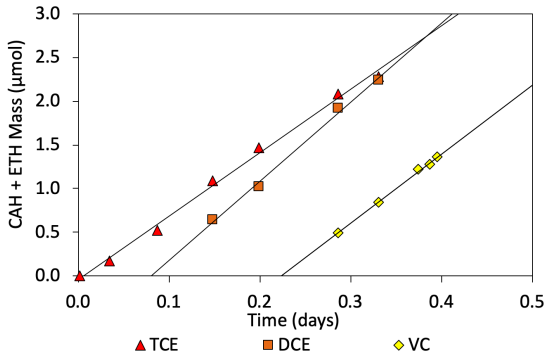

Figure 28: Converted linear rates of degradation of chlorinated ethenes for encapsulated cells in set 3. Data points represent experimental data from bottle 1. Black lines represent linear trends. Set 3 encapsulated cells were done in triplicate. Figures 61 and 65 show the other two bottles for encapsulated cells.

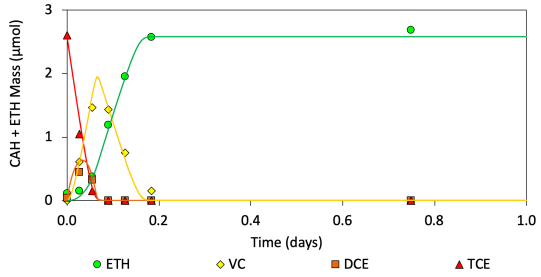

Figure 29: Model (km) rates of degradation of chlorinated ethenes for suspended cells in set 3. Data points represent experimental data from bottle 1. Solid lines represent model prediction. Set 3 suspended cells were done in triplicate. Figures 62 and 66 show the other two bottles for modeled suspended cells.

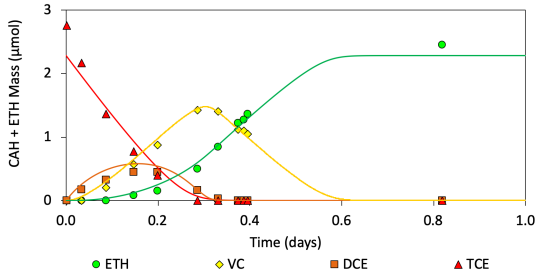

Figure 30: Model (km) rates of degradation of chlorinated ethenes for encapsulated cells in set 3. Data points represent experimental data from bottle 1. Solid lines represent model prediction. Set 3 encapsulated cells were done in triplicate. Figures 63 and 67 show the other two bottles for modeled encapsulated cells.

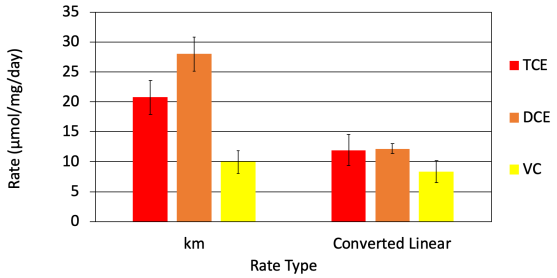

Figure 31: Rates of chlorinated ethene degradation for set 3 suspended cells. Bars represent an average of three bottles. Error bars represent standard deviation between the three bottles. km represents non-linear sum of least squared errors model which accounts for inhibition while converted linear rates do not.

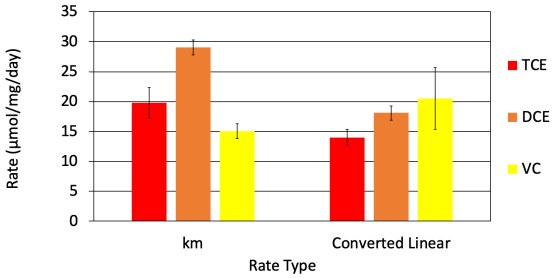

Figure 32: Rates of chlorinated ethene degradation for set 2 encapsulated cells. Bars represent an average of three trials. Error bars represent standard deviation between three trials. km represents non-linear sum of least squared errors model which accounts for inhibition while converted linear rates do not.

Encapsulated cells were cured for 1 hour in set 3 just like set 2. Varying levels of gel matrix degradation were still seen (Figure 33). Bead diameters for the 3rd set of encapsulated cells ranged from 1-3 mm in diameter. Some beads became oblong or irregular in shape. All bottles in which the beads in Figure 33 came from were cloudy suggesting some alginate had dissolved into the bulk solution which aligns with what was seen in the bottles for sets 1 and 2.

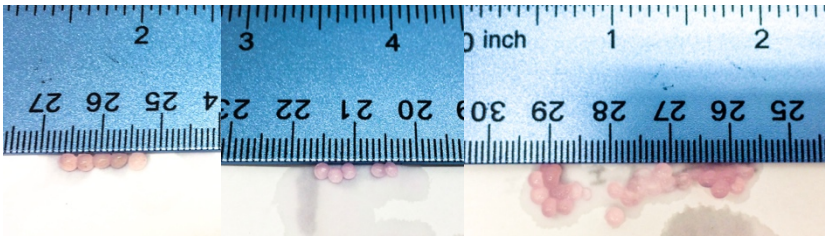

Figure 33: Three different biotic bottles with varying levels of bead degradation shown against a ruler for scale. Some beads were still 2-3 mm in diameter (left) while others were ~1.5-2 mm in diameter (middle), and others became oblong in shape with diameters ranging from 1-3 mm (right). Pink color is from resazurin indicator. Photos were taken 4 months after beads were created.

Set 4 – Suspended VS Encapsulated (Oxygen Exposed)

Rates of dechlorination for oxygen exposed beads and suspended cells were lower than non-exposed cells (Figures 34, 35, 36, 37, 38, 39). The sodium alginate matrix did not protect the cells from damage at an oxygen concentration of 0.97%. Oxygen exposed beads appeared to perform better than suspended cells when exposed to oxygen; however, there was insufficient data

to determine if the dechlorination rates between suspended and encapsulated cells were statistically significant (Figures 38, 39). In addition, modeled (km) rates of degradation were lower than converted linear rates likely due to the fact that oxygen inhibition is not included in the model.

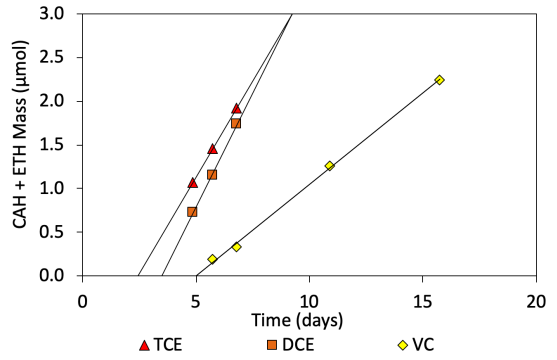

Figure 34: Converted linear rates of degradation of chlorinated ethenes for suspended cells exposed to 0.97% oxygen in the headspace in set 4. Data points represent experimental data from bottle 1. Black lines represent linear trends. Set 4 suspended cells were done in triplicate. Figures 68 and 72 show the other two bottles for suspended cells.

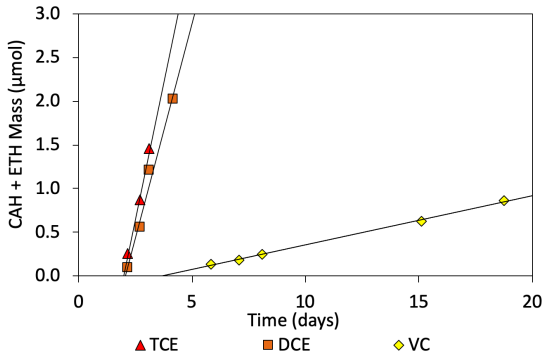

Figure 35: Converted linear rates of degradation of chlorinated ethenes for encapsulated cells exposed to 0.97% oxygen in the headspace in set 4. Data points represent experimental data from bottle 1. Black lines represent linear trends. Set 4 encapsulated cells were done in triplicate. Figures 69 and 73 show the other two bottles for encapsulated cells.

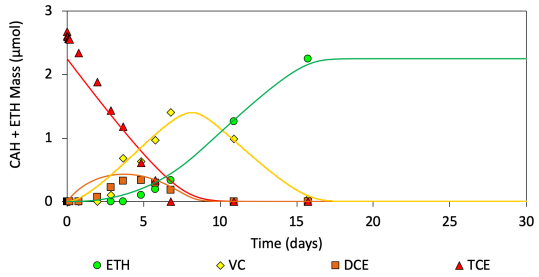

Figure 36: Model (km) rates of degradation of chlorinated ethenes for suspended cells exposed to 0.97% oxygen in the headspace for set 4. Data points represent experimental data from bottle 1. Solid lines represent model prediction. Set 4 suspended cells were done in triplicate. Figures 70 and 74 show the other two bottles for modeled suspended cells.

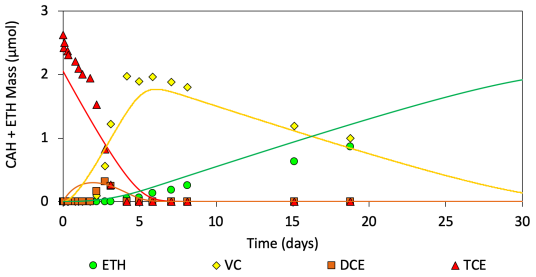

Figure 37: Model (km) rates of degradation of chlorinated ethenes for encapsulated cells exposed to 0.97% oxygen in the headspace for set 4. Data points represent experimental data from bottle 1. Solid lines represent model prediction. Set 4 encapsulated cells were done in triplicate. Figures 71 and 75 show the other two bottles for modeled encapsulated cells.

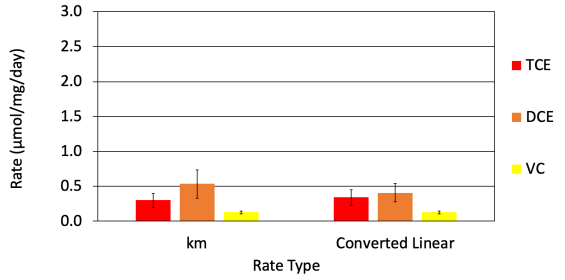

Figure 38: Set 4 suspended cells exposed to 0.97% oxygen in the headspace. Bars represent an average of three bottles. Error bars represent standard deviation between bottles. km represents non-linear sum of least squared errors model which accounts for inhibition while converted linear rates do not.

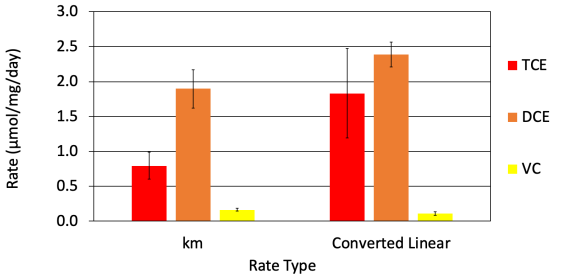

Figure 39: Set 4 suspended cells exposed to 0.97% oxygen in the headspace. Bars represent an average of three bottles. Error bars represent standard deviation between bottles. km represents non-linear sum of least squared errors model which accounts for inhibition while converted linear rates do not.

Set 1 and 2 – Multiple additions of TCE

Set 1 received five additions of TCE (Figures 40, 41). Suspended cells in set 1 were done in triplicate for the multiple additions. Encapsulated cells for set 1 were done in duplicate for multiple additions of TCE. However, encapsulated bottles appeared cloudy after two weeks suggesting cells had entered suspension from the breakdown of the alginate matrix by the time the third spike of TCE was given. Despite this, suspended and encapsulated cells appeared to perform similarly suggesting that even after encapsulation, *Dehalococcoides mccartyi* have the potential to maintain TCE degradation rates.

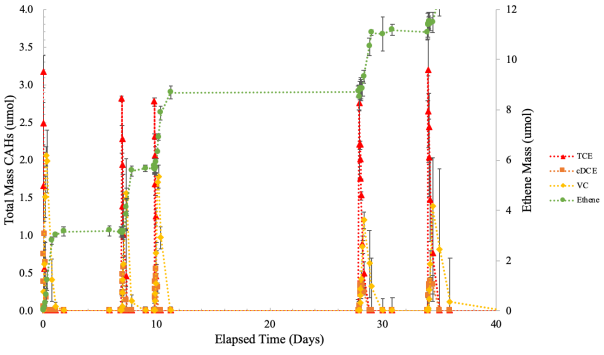

Figure 40: Set 1 suspended cells in triplicate that received multiple additions of TCE. Data points represent experimental data. Dashed lines are a visual aid to follow trends. Error bars present the standard deviation between three bottles.

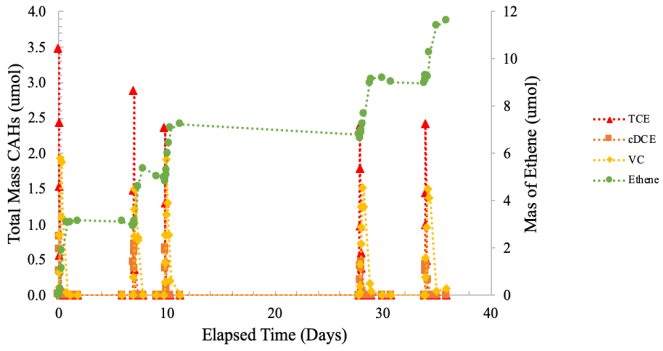

Figure 41: Set 1 encapsulated cells in duplicate that received multiple additions of TCE. Data points represent experimental data. Dashed lines are a visual aid to follow trends.

Set 2 received two additions of TCE (Figures 43). Suspended and encapsulated cells in set 2 were done in triplicate for the multiple additions of TCE. However, as discussed previously, suspended cells for set 2 were exposed to oxygen and had reduced performance as a result. Due to this fact, set 2 encapsulated cells were compared to the suspended cells for set 1. Similar to results of set 1, set 2 encapsulated cells had a similar performance to set 1 suspended cells (Figures 42, 43). This again suggests *Dehalococcoides mccartyi* is resilient after encapsulation.

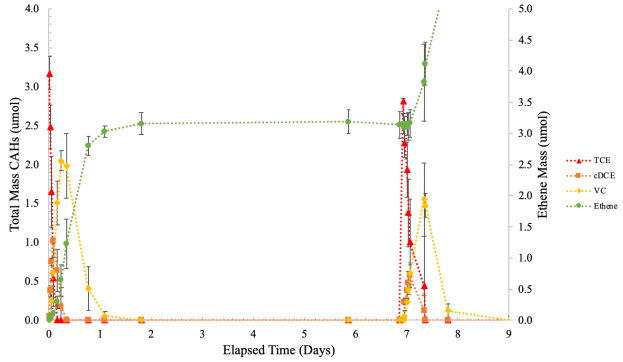

Figure 42: Set 1 suspended cells that received multiple additions of TCE on a shorted time axis. Data points represent experimental data. Dash lines are a visual aid for viewing trends. Error bars represent the standard deviation between three bottles.

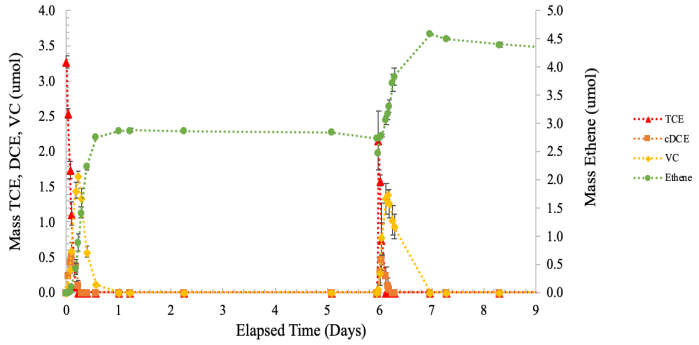

Figure 43: Set 2 encapsulated cells in triplicate that received two additions of TCE. Data points represent experimental data. Dashed linear are a visual aid to follow trends. Error bars represent the standard deviation between three bottles.

Conclusions

The *Dehalococcoides mccartyi* mixed culture can be encapsulated in a 2% wt sodium alginate gel matrix without large reductions in dechlorination rates. However, due to gel stability, encapsulation with sodium alginate is not viable in the long term. Preliminary evidence from control bottles suggest that the growth of cells may play a part in destroying the gel matrix. The gel matrix did not protect the anaerobic cells from a headspace of 0.97% oxygen as seen by the drop in dechlorination rates once exposed. There was insufficient data to tell if encapsulated cells exposed to oxygen performed significantly better than suspended cells exposed to oxygen. This study led to the following conclusions…

- A method was successfully developed to encapsulate *Dehalococcoides mccartyi* in an alginate gel matrix by fabrication in an anaerobic glove box
- Encapsulation was reproducible as indicated by similar rates of chlorinated ethene degradation from three batches of cells.
- Diffusion of chlorinated ethenes in and out of gel matrix did not inhibit the reductive dehalogenation process.
- Encapsulated *Dehalococcoides mccartyi* was not protected from 0.97% oxygen in the headspace and experienced a decline in chlorinated ethene degradation rates.
- Encapsulated cells began to break apart after 2 weeks and the alginate began to dissolve back into the bulk solution.
- Encapsulated cells are able to transform multiple additions of TCE with similar performance to suspended cells.

Future Work

Future experiments will aim to address the stability of the sodium alginate gel matrix. This could be done by changing the makeup of the media to remove anti-chelating agents or adding additional chemicals to increase stability. Literature suggests that polyethyleneimine, glutaraldehyde, polyvinyl alcohol or partial drying may be used to increase stability of the gel matrix[28]. Furthermore, attempts of covalently cross-link alginate rather than ionically cross-link the alginate may be more successful for long term stability of the gel matrix[27]. Studies using gellen gum have also found long term viability for aerobically encapsulated bacteria[36]. Once bead stability has been established, future work investigating the rebound potentially for encapsulated cells versus suspended cells once exposed to oxygen can be investigated. Potential projects that could stem from this work include the testing of anaerobic beads in flow conditions as well as full scale well testing.

Literature Cited

(1) *In Situ Remediation of Chlorinated Solvent Plumes*; Ward, C. H., Stroo, H. F., Eds.; SERDP and ESTCP remediation technology monograph series; Springer: New York, 2010.

(2) CDC | Facts About Phosgene https://emergency.cdc.gov/agent/phosgene/basics/facts.asp (accessed Apr 17, 2019).

(3) Dieter, H. H.; Kerndorff, H. Presence and Importance of Organochlorine Solvents and Other Compounds in Germany's Groundwater and Drinking Water. *Ann. Ist. Super. Sanita* **1993**, *29* (2), 263–277.

(4) Gossett, J. M. Measurement of Henry's Law Constants for C1 and C2 Chlorinated Hydrocarbons. *Environ. Sci. Technol.* **1987**, *21* (2), 202–208. https://doi.org/10.1021/es00156a012.

(5) Huling, S.; Weaver, J. Ground Water Issue: Dense Nonaqueous Phase Liquids. *EPA* **1991**, 21.

(6) Current Intelligence Bulletin 2 - Trichloroethylene (TCE) (with Reference Package). *Natl. Institue Occup. Saf. Health NIOSH* **1975**. https://doi.org/10.26616/NIOSHPUB781272.

(7) McDaniel, T. V.; Martin, P. A.; Ross, N.; Brown, S.; Lesage, S.; Pauli, B. D. Effects of Chlorinated Solvents on Four Species of North American Amphibians. *Arch. Environ. Contam. Toxicol.* **2004**, *47* (1), 101–109.

(8) Superfund History | Superfund | US EPA https://www.epa.gov/superfund/superfund-history (accessed Apr 17, 2019).

(9) Larson, D.; Consultants, G. Introduction to In-Situ Chemical Oxidation. 45.

(10) Vidonish, J. E.; Zygourakis, K.; Masiello, C. A.; Sabadell, G.; Alvarez, P. J. J. Thermal Treatment of Hydrocarbon-Impacted Soils: A Review of Technology Innovation for Sustainable Remediation. *Engineering* **2016**, *2* (4), 426–437. https://doi.org/10.1016/J.ENG.2016.04.005.

(11) EPA. A Citizen's Guide to Soil Vapor Extraction and Air Sparging. United States Environmental Protection Agency September 2012.

(12) National Research Council. *Alternatives for Ground Water Cleanup*; The National Academies Press: Washington, DC, 1994. https://doi.org/10.17226/2311.

(13) Li, B.; Lin, K.; Zhang, W.; Lu, S.; Liu, Y. Effectiveness of Air Stripping, Advanced Oxidation, and Activated Carbon Adsorption-Coupled Process in Treating Chlorinated Solvent; Contaminated Groundwater. *J. Environ. Eng.* **2012**, *138* (9), 903–914. https://doi.org/10.1061/(ASCE)EE.1943-7870.0000557.

(14) Rolston, H. M. *Experimental demonstration and modeling of aerobic cometabolism of 1,4-dioxane by isobutane-utilizing microorganisms in aquifer microcosms*; Oregon State University, 2017.

(15) Tyagi, M.; da Fonseca, M. M. R.; de Carvalho, C. C. C. R. Bioaugmentation and Biostimulation Strategies to Improve the Effectiveness of Bioremediation Processes. *Biodegradation* **2011**, *22* (2), 231–241. https://doi.org/10.1007/s10532-010-9394-4.

(16) Kennedy, L. G.; Everett, J. W.; Becvar, E.; DeFeo, D. Field-Scale Demonstration of Induced Biogeochemical Reductive Dechlorination at Dover Air Force Base, Dover, Delaware. *J. Contam. Hydrol.* **2006**, *88* (1), 119–136. https://doi.org/10.1016/j.jconhyd.2006.06.007.

(17) Nzila, A.; Razzak, S. A.; Zhu, J. Bioaugmentation: An Emerging Strategy of Industrial Wastewater Treatment for Reuse and Discharge. *Int. J. Environ. Res. Public. Health* **2016**, *13* (9), 846. https://doi.org/10.3390/ijerph13090846.
(18) Ellis, D. E.; Lutz, E. J.; Odom, J. M.; Buchanan, R. J.; Bartlett, C. L.; Lee, M. D.; Harkness, M. R.; DeWeerd, K. A. Bioaugmentation for Accelerated In Situ Anaerobic Bioremediation. *Environ. Sci. Technol.* **2000**, *34* (11), 2254–2260. https://doi.org/10.1021/es990638e.
(19) Coleman, N. V.; Mattes, T. E.; Gossett, J. M.; Spain, J. C. Biodegradation of Cis-Dichloroethene as the Sole Carbon Source by a Beta-Proteobacterium. *Appl. Environ. Microbiol.* **2002**, *68* (6), 2726–2730. https://doi.org/10.1128/aem.68.6.2726-2730.2002.
(20) Coleman, N. V.; Mattes, T. E.; Gossett, J. M.; Spain, J. C. Phylogenetic and Kinetic Diversity of Aerobic Vinyl Chloride-Assimilating Bacteria from Contaminated Sites. *Appl. Environ. Microbiol.* **2002**, *68* (12), 6162–6171. https://doi.org/10.1128/aem.68.12.6162-6171.2002.
(21) Kruse, T.; van de Pas, B. A.; Atteia, A.; Krab, K.; Hagen, W. R.; Goodwin, L.; Chain, P.; Boeren, S.; Maphosa, F.; Schraa, G.; et al. Genomic, Proteomic, and Biochemical Analysis of the Organohalide Respiratory Pathway in Desulfitobacterium Dehalogenans. *J. Bacteriol.* **2015**, *197* (5), 893. https://doi.org/10.1128/JB.02370-14.
(22) Hug, L. A.; Maphosa, F.; Leys, D.; Löffler, F. E.; Smidt, H.; Edwards, E. A.; Adrian, L. Overview of Organohalide-Respiring Bacteria and a Proposal for a Classification System for Reductive Dehalogenases. *Philos. Trans. R. Soc. Lond. B. Biol. Sci. 368* (1616), 20120322–20120322. https://doi.org/10.1098/rstb.2012.0322.
(23) Mayer-Blackwell, K.; Azizian, M. F.; Green, J. K.; Spormann, A. M.; Semprini, L. Survival of Vinyl Chloride Respiring Dehalococcoides Mccartyi under Long-Term Electron Donor Limitation. *Environ. Sci. Technol.* **2017**, *51* (3), 1635–1642. https://doi.org/10.1021/acs.est.6b05050.
(24) Hentges, D. J. Anaerobes: General Characteristics. In *Medical Microbiology*; Baron, S., Ed.; University of Texas Medical Branch at Galveston: Galveston (TX), 1996.
(25) Amos, B. K.; Ritalahti, K. M.; Cruz-Garcia, C.; Padilla-Crespo, E.; Löffler, F. E. Oxygen Effect on Dehalococcoides Viability and Biomarker Quantification. *Environ. Sci. Technol.* **2008**, *42* (15), 5718–5726. https://doi.org/10.1021/es703227g.
(26) Major, D. W.; McMaster, M. L.; Cox, E. E.; Edwards, E. A.; Dworatzek, S. M.; Hendrickson, E. R.; Starr, M. G.; Payne, J. A.; Buonamici, L. W. Field Demonstration of Successful Bioaugmentation To Achieve Dechlorination of Tetrachloroethene To Ethene. *Environ. Sci. Technol.* **2002**, *36* (23), 5106–5116. https://doi.org/10.1021/es0255711.
(27) Lee, K. Y.; Mooney, D. J. Alginate: Properties and Biomedical Applications. *Prog. Polym. Sci.* **2012**, *37* (1), 106–126. https://doi.org/10.1016/j.progpolymsci.2011.06.003.
(28) Willaert, R. Cell Immobilization and Its Applications in Biotechnology; 2011; pp 313–367. https://doi.org/10.1201/b11490-13.
(29) Frascari, D.; Zanaroli, G.; Danko, A. S. In Situ Aerobic Cometabolism of Chlorinated Solvents: A Review. *J. Hazard. Mater.* **2015**, *283*, 382–399. https://doi.org/10.1016/j.jhazmat.2014.09.041.
(30) Moslemy, P.; Neufeld, R. J.; Millette, D.; Guiot, S. R. Transport of Gellan Gum Microbeads through Sand: An Experimental Evaluation for Encapsulated Cell Bioaugmentation. *J. Environ. Manage.* **2003**, *69* (3), 249–259. https://doi.org/10.1016/j.jenvman.2003.09.003.

(31) Petrich, C. R.; Stormo, K. E.; Ralston, D. R.; Crawford, R. L. Encapsulated Cell Bioremediation: Evaluation on the Basis of Particle Tracer Tests. *Groundwater* **1998**, *36* (5), 771–778. https://doi.org/10.1111/j.1745-6584.1998.tb02194.x.
(32) McLoughlin, A. J. Controlled Release of Immobilized Cells as a Strategy to Regulate Ecological Competence of Inocula. In *Biotechnics/Wastewater. Advances in Biochemical Engineering/Biotechnology*; Springer-Verlag: Berlin; New York, 1994; Vol. 51, pp 1–45.
(33) Yang, Y.; McCarty, P. L. Competition for Hydrogen within a Chlorinated Solvent Dehalogenating Anaerobic Mixed Culture. *Environ. Sci. Technol.* **1998**, *32* (22), 3591–3597. https://doi.org/10.1021/es980363n.
(34) Hendrickson, E. R.; Payne, J. A.; Young, R. M.; Starr, M. G.; Perry, M. P.; Fahnestock, S.; Ellis, D. E.; Ebersole, R. C. Molecular Analysis of Dehalococcoides 16S Ribosomal DNA from Chloroethene-Contaminated Sites throughout North America and Europe. *Appl. Environ. Microbiol.* **2002**, *68* (2), 485–495. https://doi.org/10.1128/AEM.68.2.485-495.2002.
(35) McCarty, P. L.; Chu, M.-Y.; Kitanidis, P. K. Electron Donor and PH Relationships for Biologically Enhanced Dissolution of Chlorinated Solvent DNAPL in Groundwater. *Situ Bioremediation* **2007**, *43* (5), 276–282. https://doi.org/10.1016/j.ejsobi.2007.03.004.
(36) Rasmussen, M. Co-Encapsulation of Slow Release Substrates and Microbial Cultures in Alginate and Gellan Gum Beads to Promote the Co-Metabolic Transformation of 1,4-Dioxane and Chlorinate Aliphatic Hydrocarbons, Oregon State University: Corvallis, OR, 2018.
(37) Molzahn, P. Batch and Continuous Flow Column Studies of Methane Consumption and Methanol Production by Methylosinus Trichosporium OB3b and Methylomicrobium Buryatense 5GB1 Immobilized In Ca-Alginate and Agarose Hydrogels, Oregon State University: Corvallis, OR, 2016.
(38) Smith, L. H.; McCarty, P. L.; Kitanidis, P. K. Spreadsheet Method for Evaluation of Biochemical Reaction Rate Coefficients and Their Uncertainties by Weighted Nonlinear Least-Squares Analysis of the Integrated Monod Equation. *Appl Env. Microbiol* **1998**, *64* (6), 2044–2050.
(39) Yu, S.; Dolan, M. E.; Semprini, L. Kinetics and Inhibition of Reductive Dechlorination of Chlorinated Ethylenes by Two Different Mixed Cultures. *Environ. Sci. Technol.* **2005**, *39* (1), 195–205. https://doi.org/10.1021/es0496773.
(40) Ehret, E. L. Inhibition of Organohalide-Respiring Bacteria by Carbon Tetrachloride and Chloroform, Oregon State University: Corvallis, OR, 2017.
(41) Sander, R. Compilation of Henry's Law Constants for Inorganic and Organic Species of Potential Importance in Environmental Chemistry. In *10 Copyright © 2010 by ASME*; 1999.
(42) Yu, S.; Semprini, L. Kinetics and Modeling of Reductive Dechlorination at High PCE and TCE Concentrations. *Biotechnol. Bioeng.* **2004**, *88* (4), 451–464. https://doi.org/10.1002/bit.20260.

Appendix A: Figures

Set 1 – Bottles 2

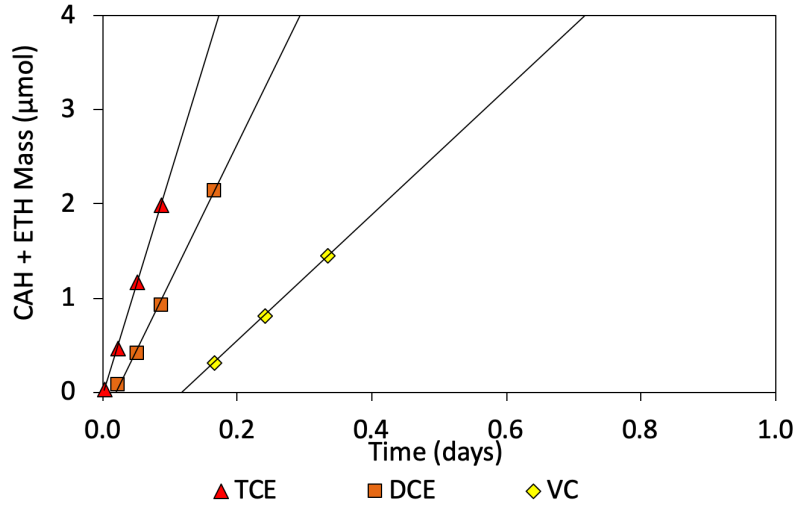

Figure 44: Suspended cells, set 1, bottle 2. Data points are representative of the total mass of CAH that has been consumed in a single trial. Black lines represent the maximum converted linear rates.

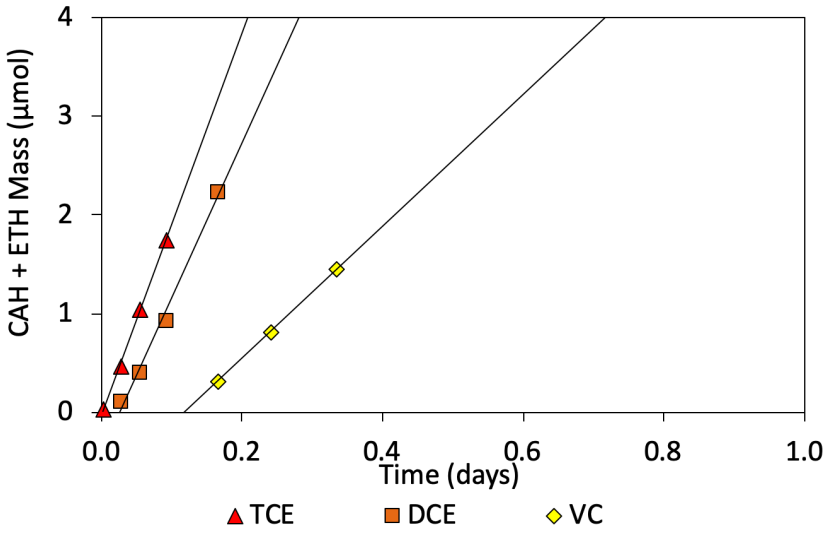

Figure 45: Encapsulated cells, set 1, bottle 2. Data points are representative of the total mass of CAH that has been consumed in a single trial. Black lines represent the maximum converted linear rates.

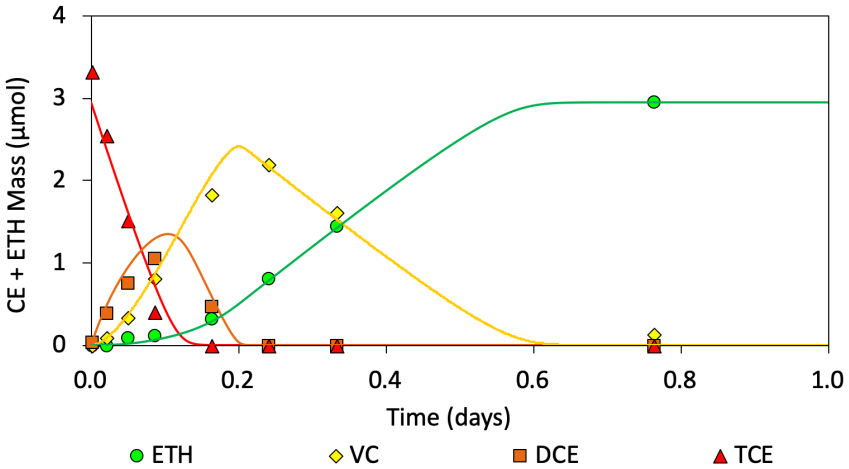

Figure 46: Suspended cells, set 1, bottle 2. Data points represent experimental data from bottle 2. Solid lines represent non-linear sum of least squared errors model prediction.

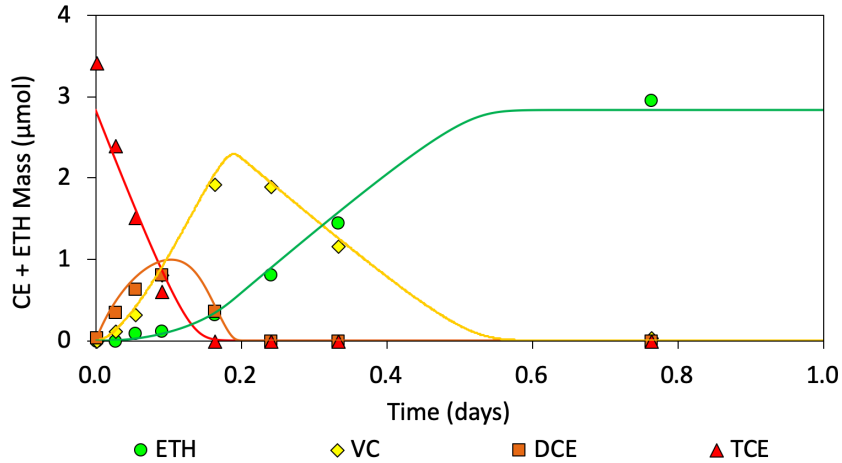

Figure 47: Encapsulated cells, set 1, bottle 2. Data points represent experimental data from bottle 2. Solid lines represent non-linear sum of least squared errors model prediction.

Set 1 – Bottles 3

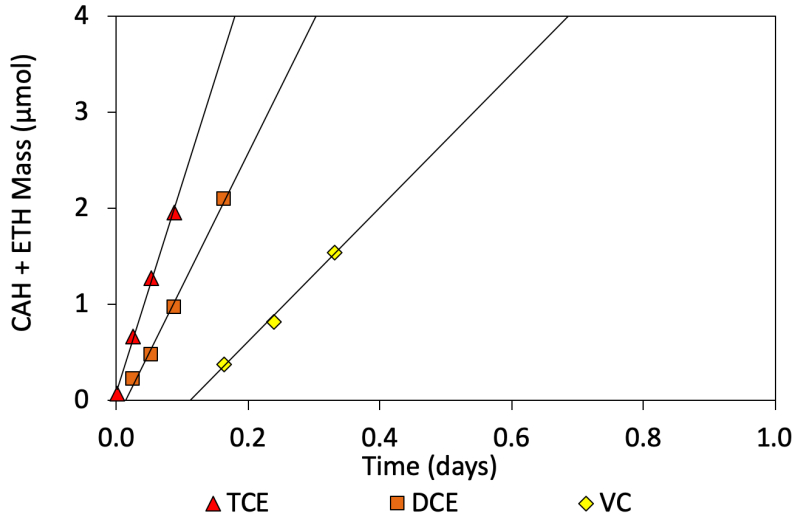

Figure 48: Suspended cells, set 1, bottle 3. Data points are representative of the total mass of CAH that has been consumed in a single trial. Black lines represent the maximum converted linear rates.

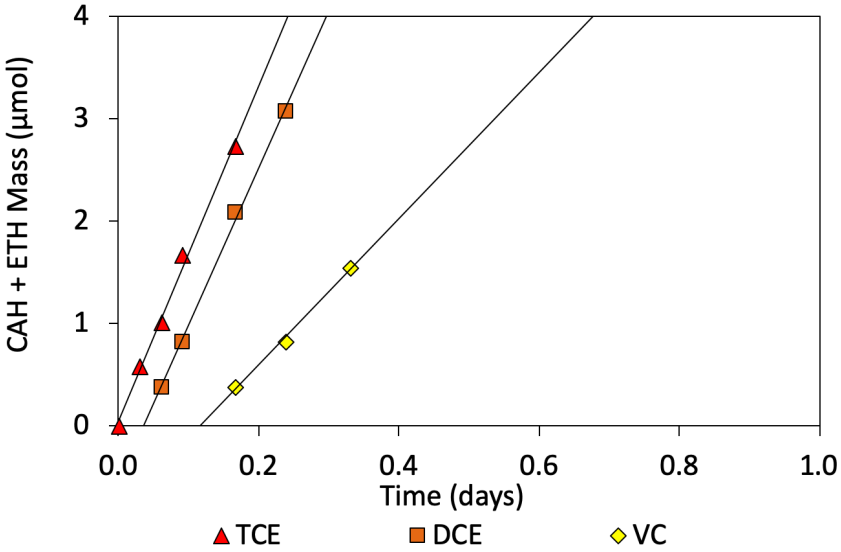

Figure 49: Encapsulated cells, set 1, bottle 3. Data points are representative of the total mass of CAH that has been consumed in a single trial. Black lines represent the maximum converted linear rates.

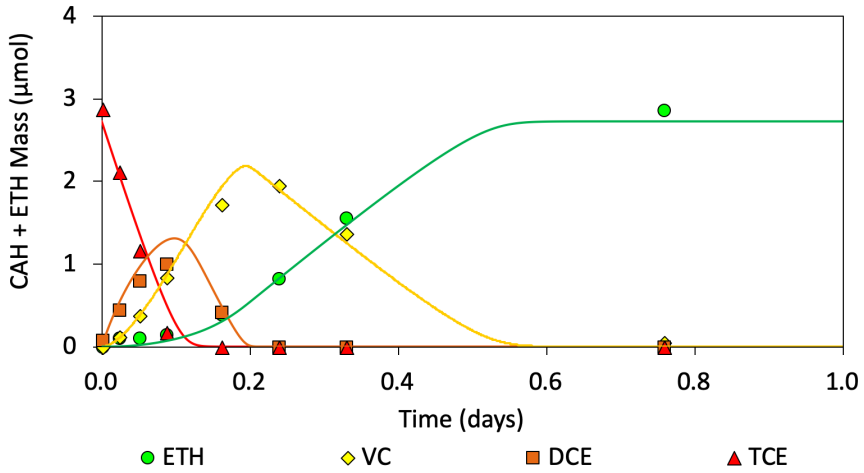

Figure 50: Suspended cells, set 1, bottle 3. Data points represent experimental data from bottle 3. Solid lines represent non-linear sum of least squared errors model prediction.

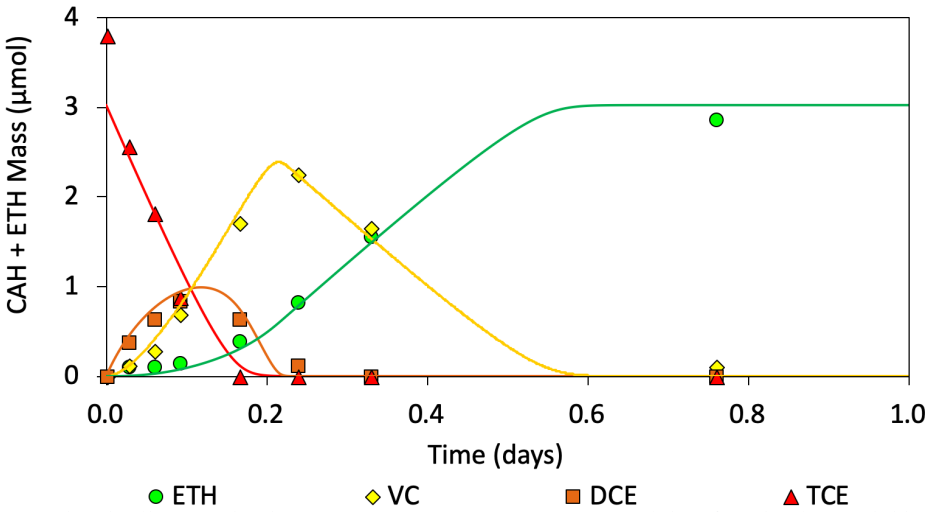

Figure 51:Encapsulated cells, set 1, bottle 3. Data points represent experimental data from bottle 3. Solid lines represent non-linear sum of least squared errors model prediction

Set 2 – Bottles 2

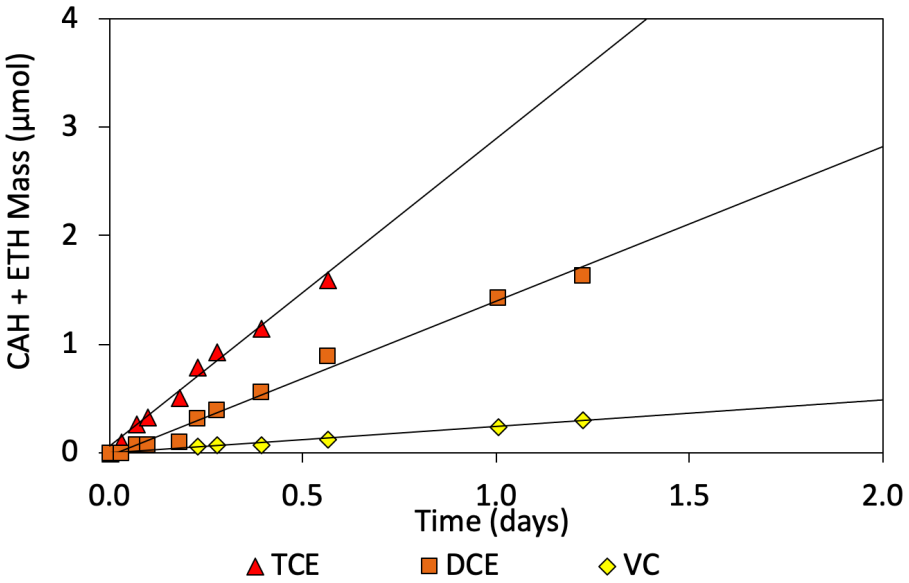

Figure 52: Suspended cells, set 2, bottle 2. Data points are representative of the total mass of CAH that has been consumed in a single trial. Black lines represent the maximum converted linear rates.

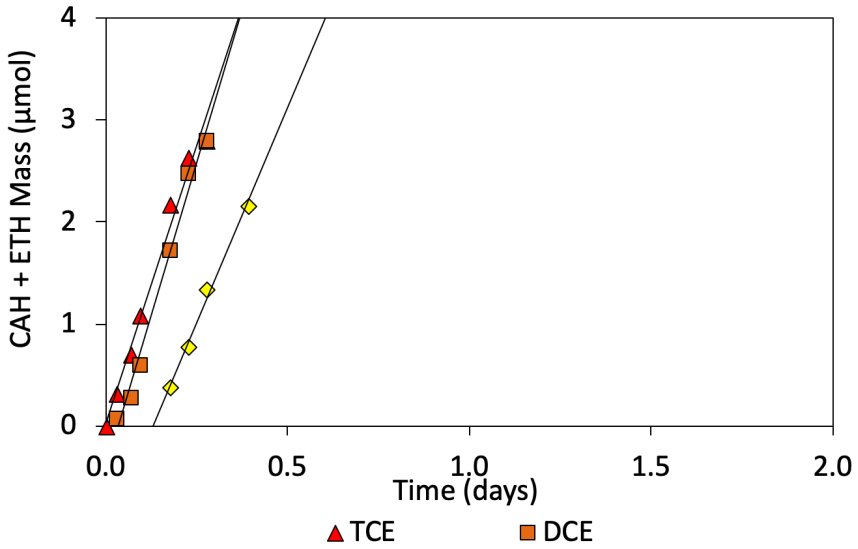

Figure 53: Encapsulated cells, set 2, bottle 2. Data points are representative of the total mass of CAH that has been consumed in a single trial. Black lines represent the maximum converted linear rates.

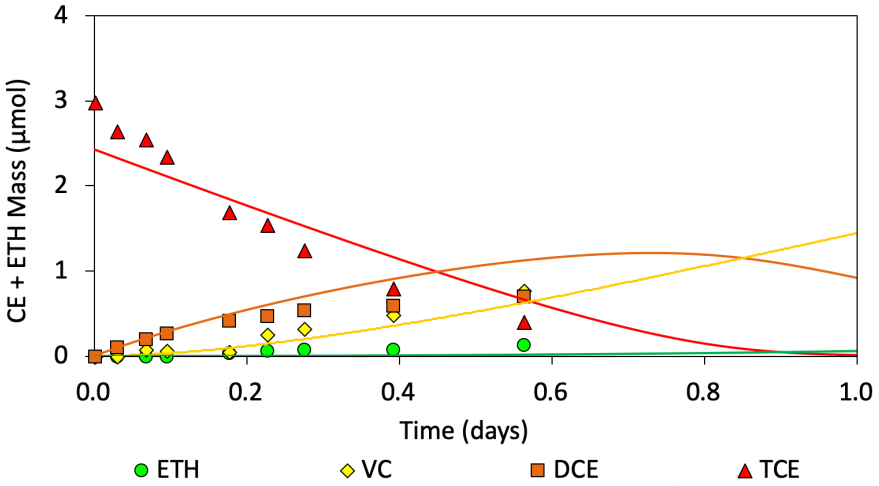

Figure 54: Suspended cells, set 2, bottle 2. Data points represent experimental data from bottle 2. Solid lines represent non-linear sum of least squared errors model prediction.

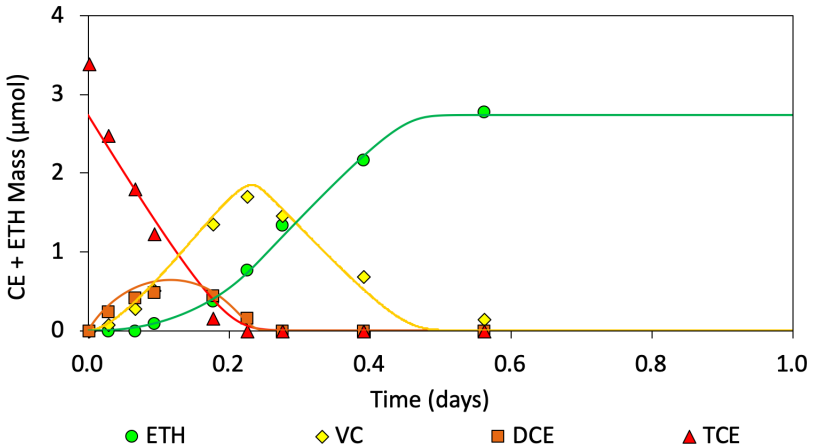

Figure 55: Encapsulated cells, set 2, bottle 2. Data points represent experimental data from bottle 2. Solid lines represent non-linear sum of least squared errors model prediction.

Set 2 – Bottles 3

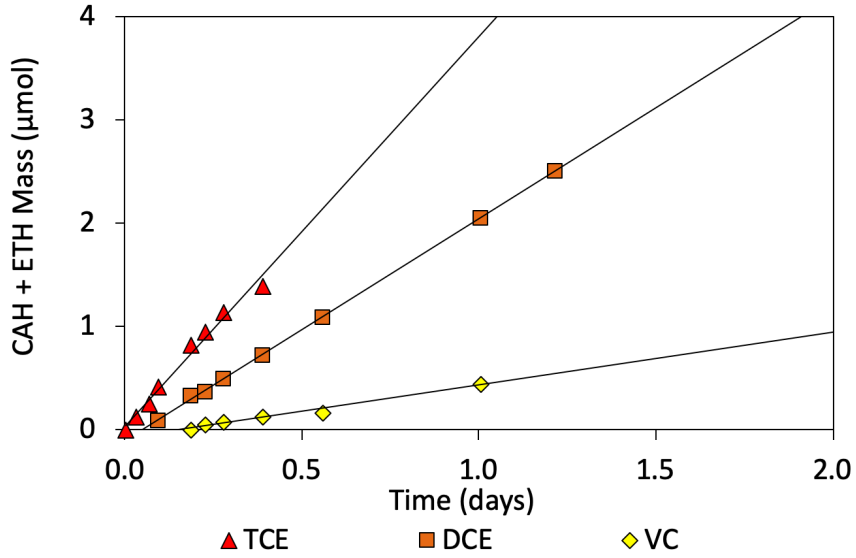

Figure 56: Suspended cells, set 2, bottle 3. Data points are representative of the total mass of CAH that has been consumed in a single trial. Black lines represent the maximum converted linear rates.

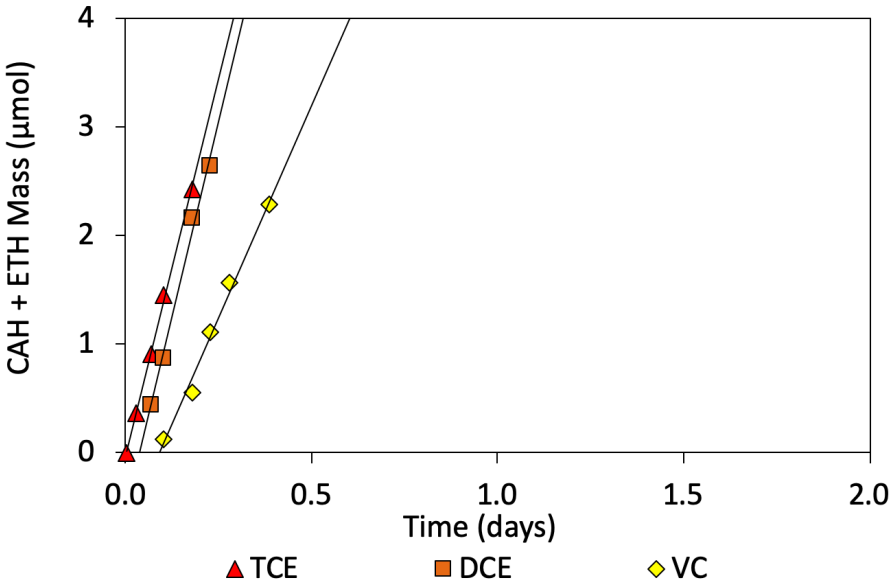

Figure 57: Encapsulated cells, set 2, bottle 3. Data points are representative of the total mass of CAH that has been consumed in a single trial. Black lines represent the maximum converted linear rates.

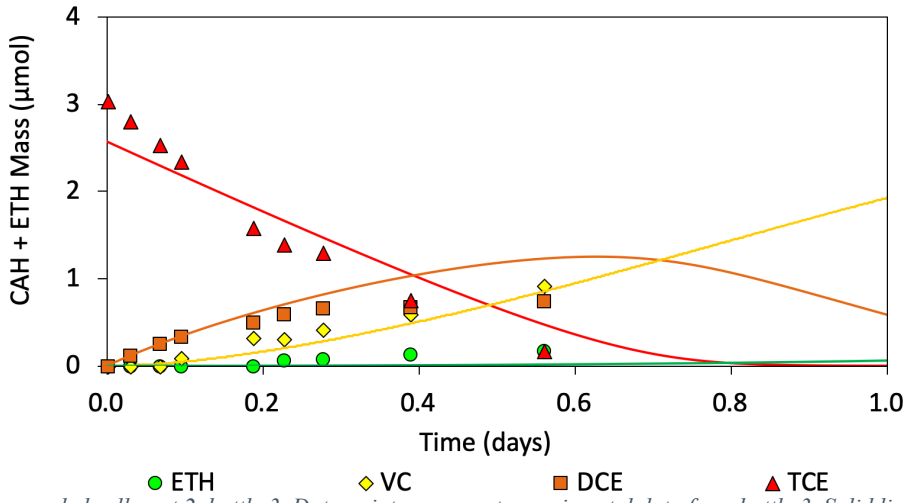

Figure 58: Suspended cells, set 2, bottle 3. Data points represent experimental data from bottle 3. Solid lines represent non-linear sum of least squared errors model prediction.

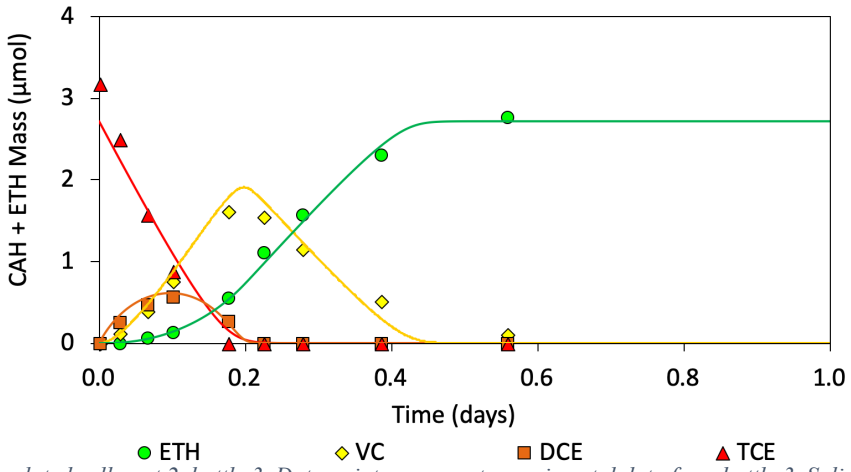

Figure 59: Encapsulated cells, set 2, bottle 3. Data points represent experimental data from bottle 3. Solid lines represent non-linear sum of least squared errors model prediction.

Set 3 – Bottles 2

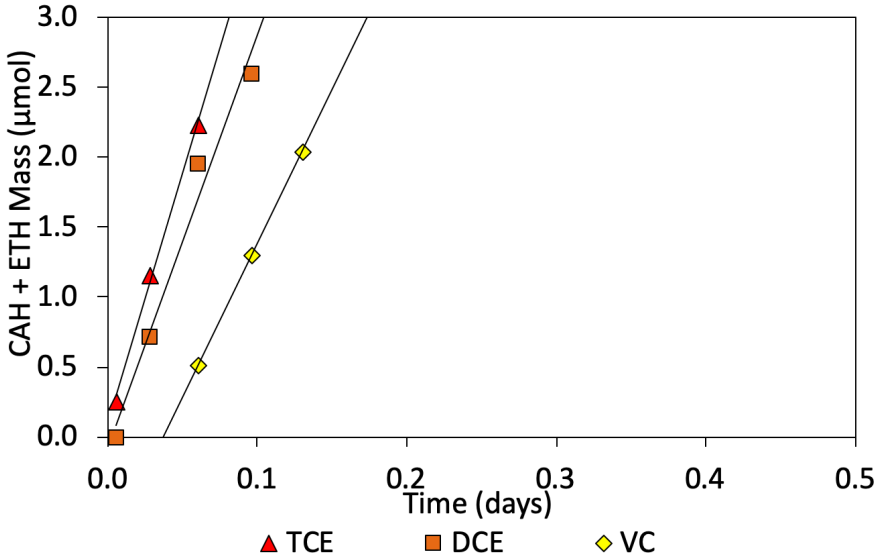

Figure 60: Suspended cells, set 3, bottle 2. Data points are representative of the total mass of CAH that has been consumed in a single trial. Black lines represent the maximum converted linear rates.

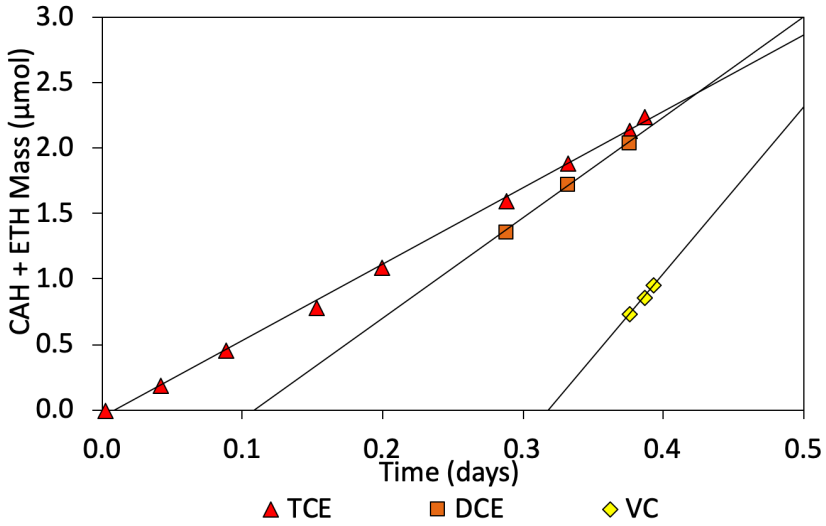

Figure 61: Encapsulated cells, set 3, bottle 2. Data points are representative of the total mass of CAH that has been consumed in a single trial. Black lines represent the maximum converted linear rates.

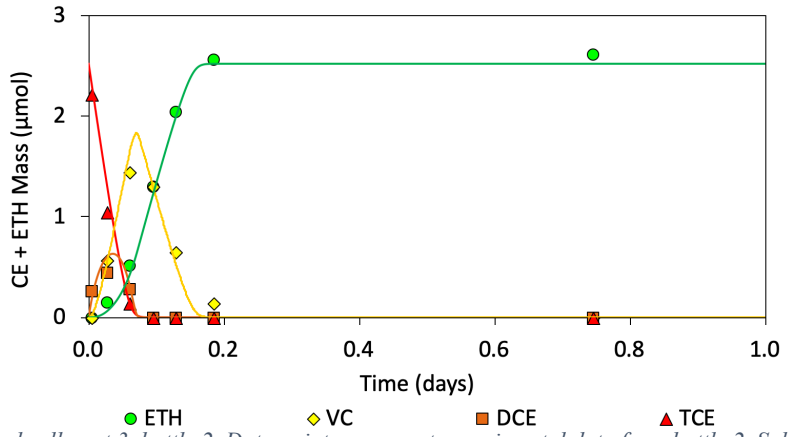

Figure 62: Suspended cells, set 3, bottle 2. Data points represent experimental data from bottle 2. Solid lines represent non-linear sum of least squared errors model prediction.

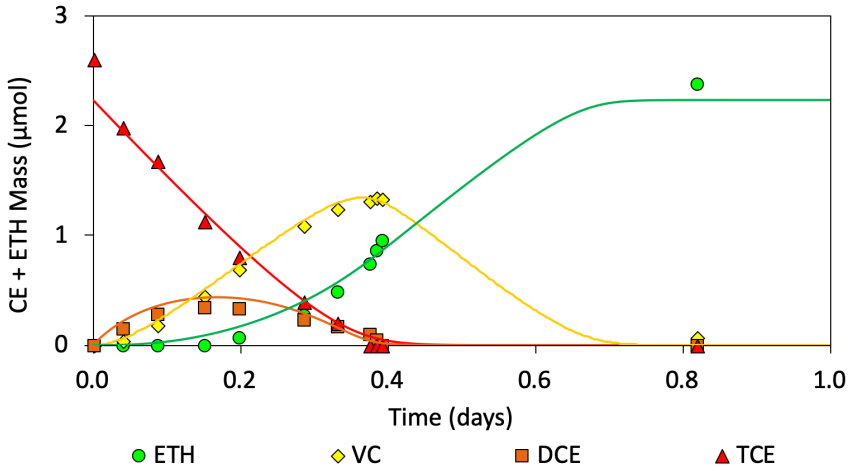

Figure 63: encapsulated cells, set 3, bottle 2. Data points represent experimental data from bottle 2. Solid lines represent non-linear sum of least squared errors model prediction.

Set 3 – Bottles 3

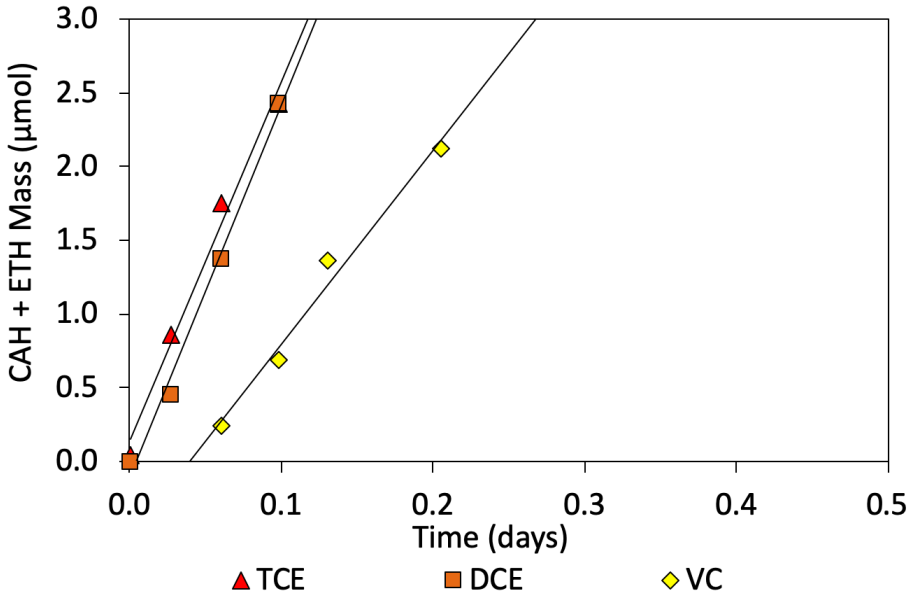

Figure 64: Suspended cells, set 3, bottle 3. Data points are representative of the total mass of CAH that has been consumed in a single trial. Black lines represent the maximum converted linear rates.

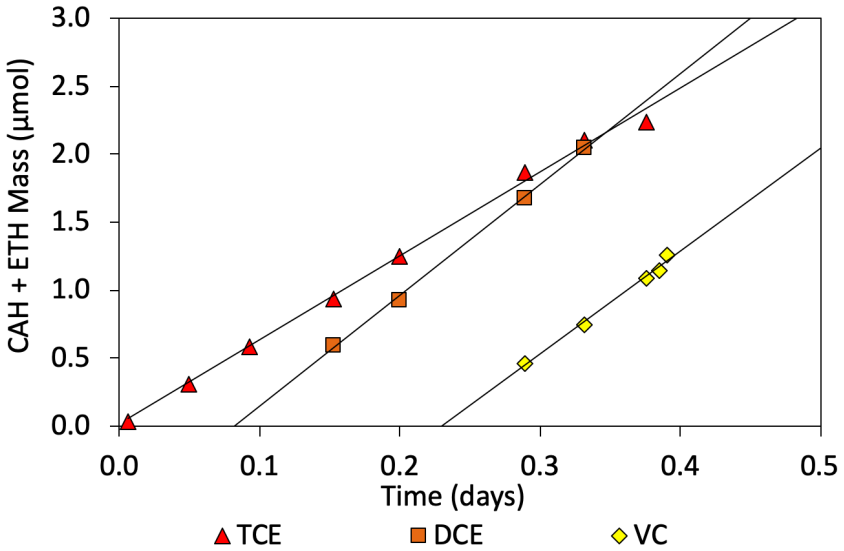

Figure 65: Encapsulated cells, set 3, bottle 3. Data points are representative of the total mass of CAH that has been consumed in a single trial. Black lines represent the maximum converted linear rates.

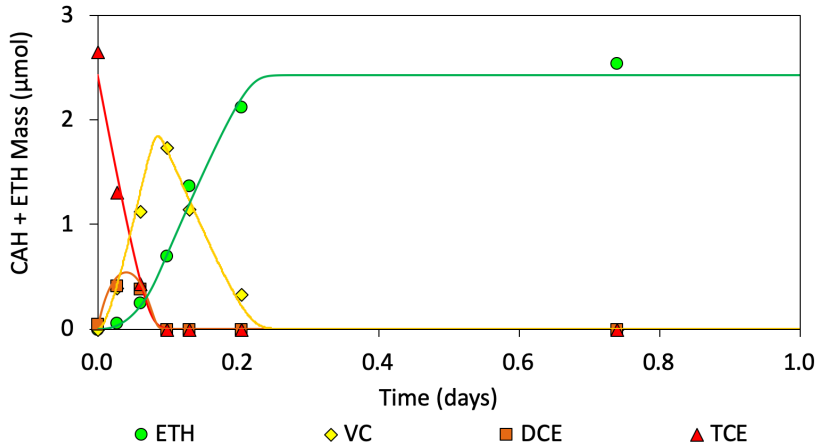

Figure 66: Suspended cells, set 3, bottle 3. Data points represent experimental data from bottle 3. Solid lines represent non-linear sum of least squared errors model prediction.

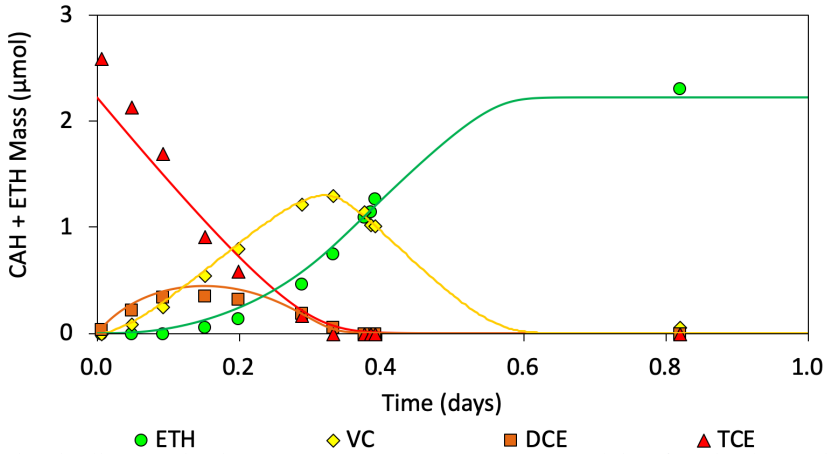

Figure 67: Encapsulated cells, set 3, bottle 3. Data points represent experimental data from bottle 3. Solid lines represent non-linear sum of least squared errors model prediction.

Set 4 – Bottles 2

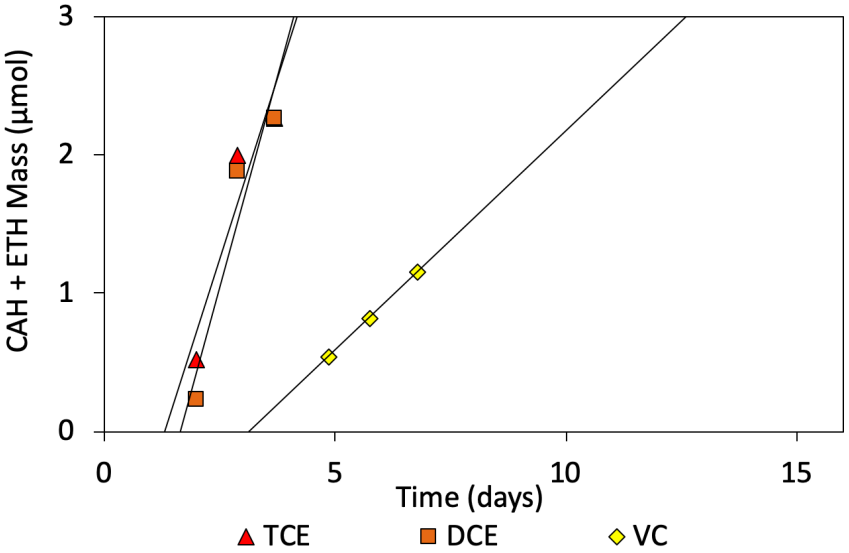

Figure 68: Suspended cells, set 4, bottle 2. Data points are representative of the total mass of CAH that has been consumed in a single trial. Black lines represent the maximum converted linear rates. Note that TCE and DCE had R^2 values of 0.873 and 0.897 respectively which are less than the desired 0.98.

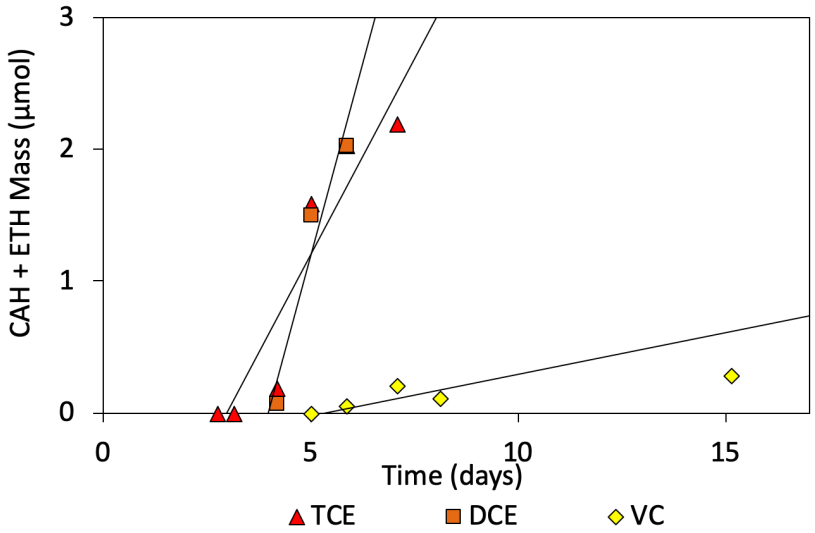

Figure 69: Encapsulated cells, set 4, bottle 2. Data points are representative of the total mass of CAH that has been consumed in a single trial. Black lines represent the maximum converted linear rates. Note that TCE, DCE, and VC all had R^2 values of 0.886, 0.923, 0.777 respectively which are less than the desired 0.98.

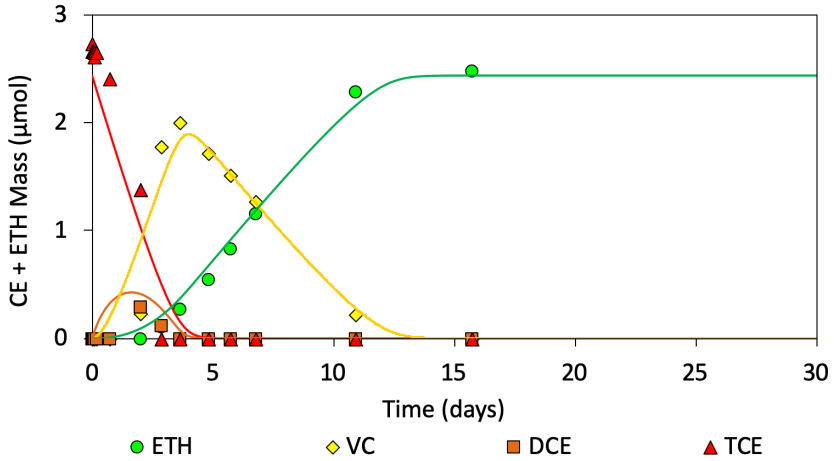

Figure 70: Suspended cells, set 4, bottle 2. Data points represent experimental data from bottle 2. Solid lines represent non-linear sum of least squared errors model prediction.

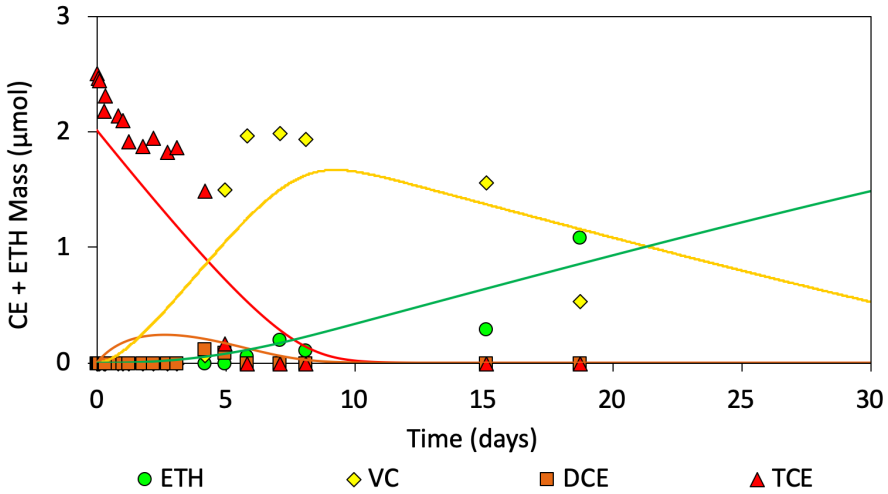

Figure 71: Encapsulated cells, set 4, bottle 2. Data points represent experimental data from bottle 2. Solid lines represent non-linear sum of least squared errors model prediction.

Set 4 – Bottles 3

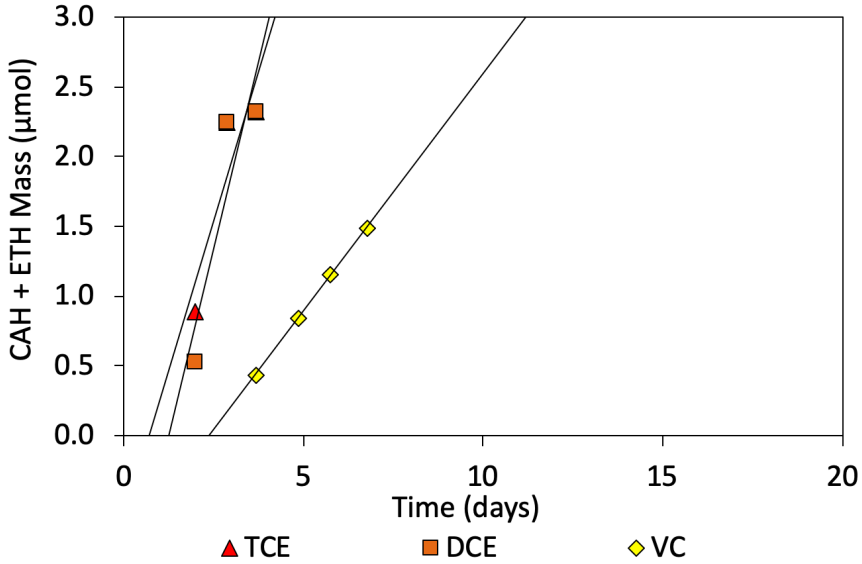

Figure 72: Suspended cells, set 4, bottle 3. Data points are representative of the total mass of CAH that has been consumed in a single trial. Black lines represent the maximum converted linear rates. Note that TCE and DCE had R^2 values of 0.803 and 0.796 respectively which are less than the desired value of 0.98.

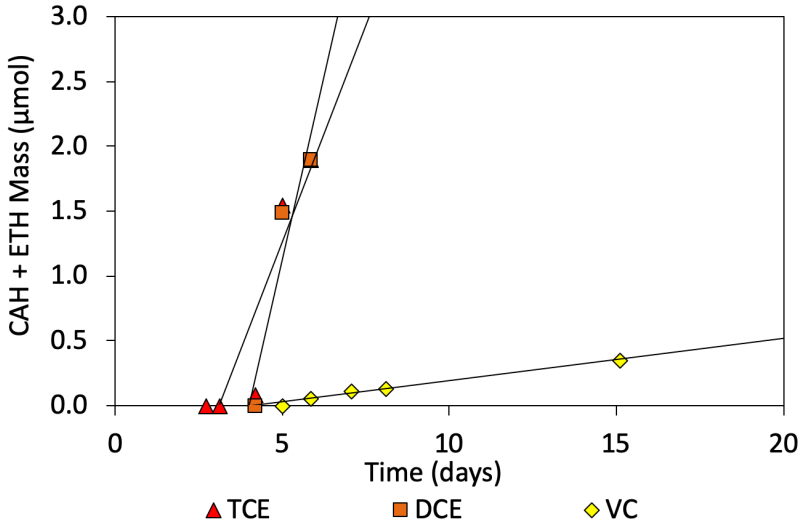

Figure 73: Encapsulated cells, set 4, bottle 3. Data points are representative of the total mass of CAH that has been consumed in a single trial. Black lines represent the maximum converted linear rates. Note that TCE and DCE had R^2 values of 0.844 and 0.890 respectively which are less than the desired values of 0.98.

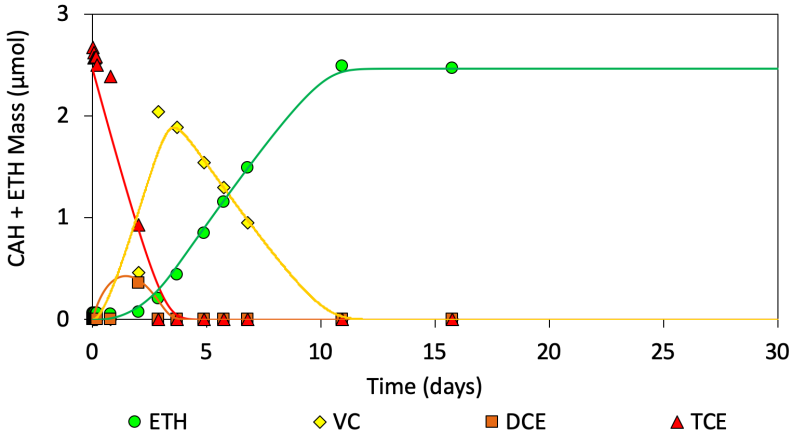

Figure 74: Suspended cells, set 4, bottle 3. Data points represent experimental data from bottle 3. Solid lines represent non-linear sum of least squared errors model prediction.

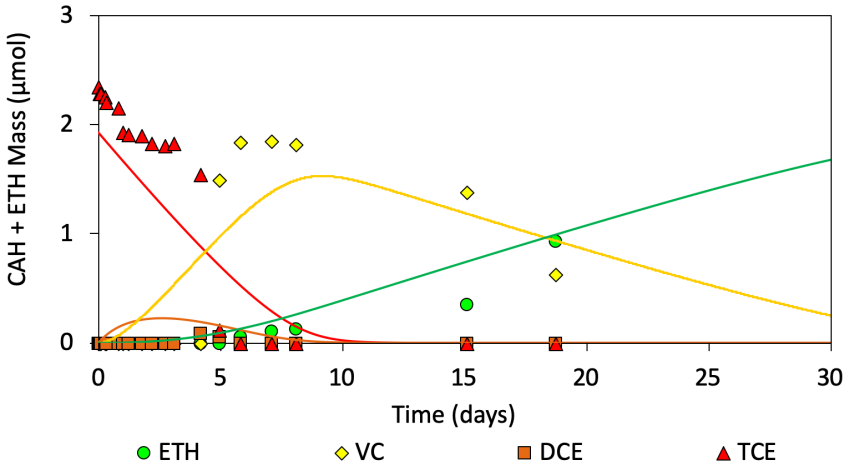

Figure 75: Encapsulated cells, set 4, bottle 3. Data points represent experimental data from bottle 3. Solid lines represent non-linear sum of least squared errors model prediction.

Standard Curves

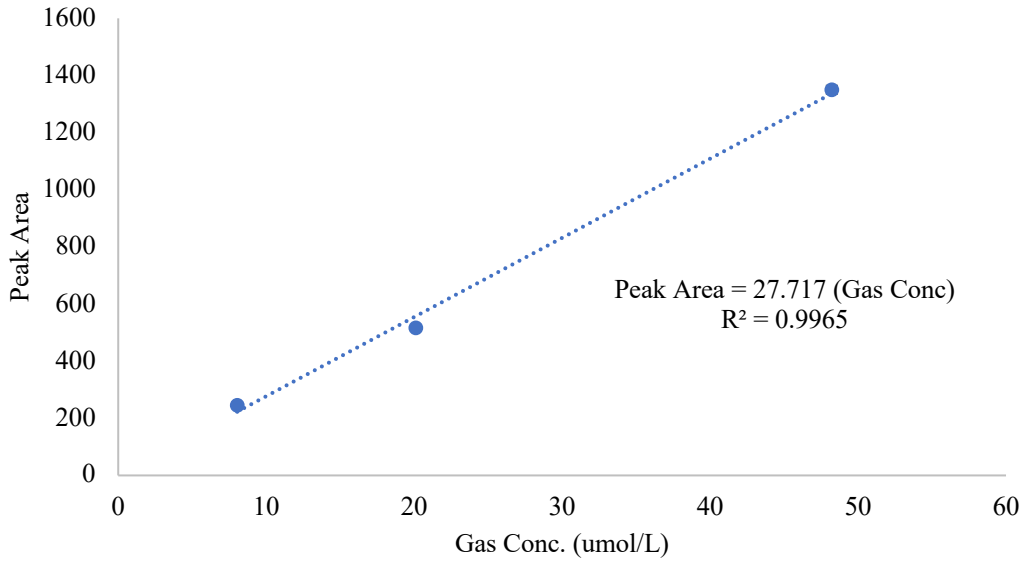

Figure 76: Standard curve for TCE on gas chromatograph. Dotted line represents linear relationship between peak area and concentration TCE in the gas phase. Data points represent an average of three trials. Error bars represent standard deviation between trials. Standard deviation small so error bars are barely visible.

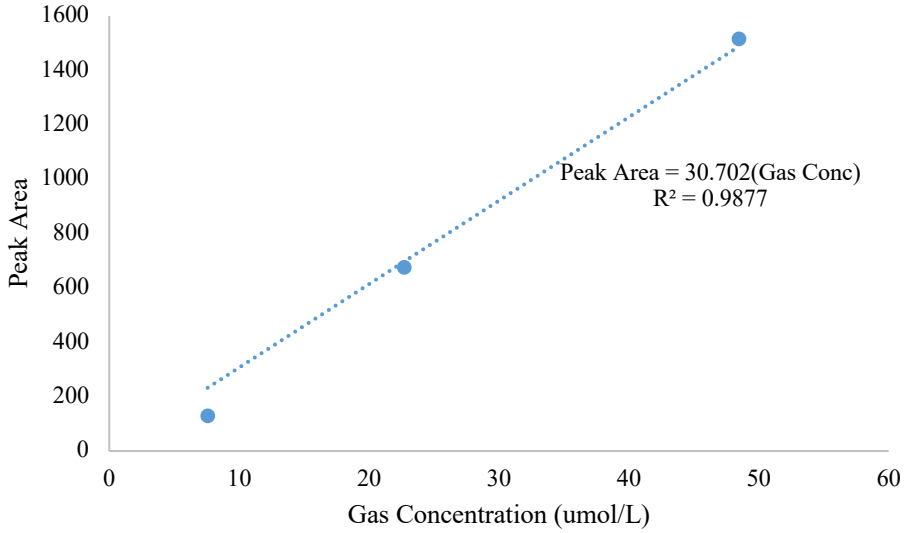

Figure 77: Standard curve for VC on gas chromatograph. Dotted line represents linear relationship between peak area and concentration VC in the gas phase. Data points represent an average of three trials. Error bars represent standard deviation between trials. Standard deviation small so error bars are barely visible.

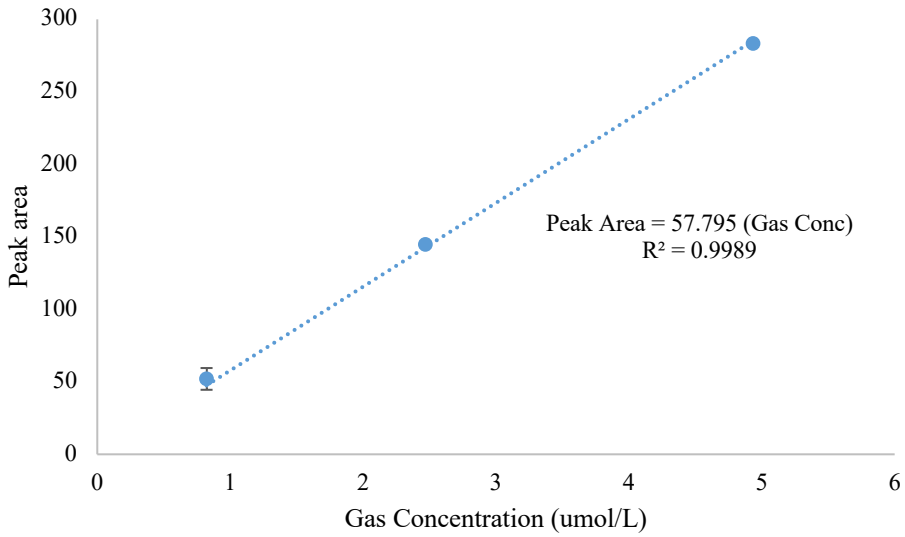

Figure 78: Standard curve for cDCE on gas chromatograph. Dotted line represents linear relationship between peak area and concentration cDCE in the gas phase. Data points represent an average of three trials. Error bars represent standard deviation between trials. Standard deviation small so error bars are barely visible.

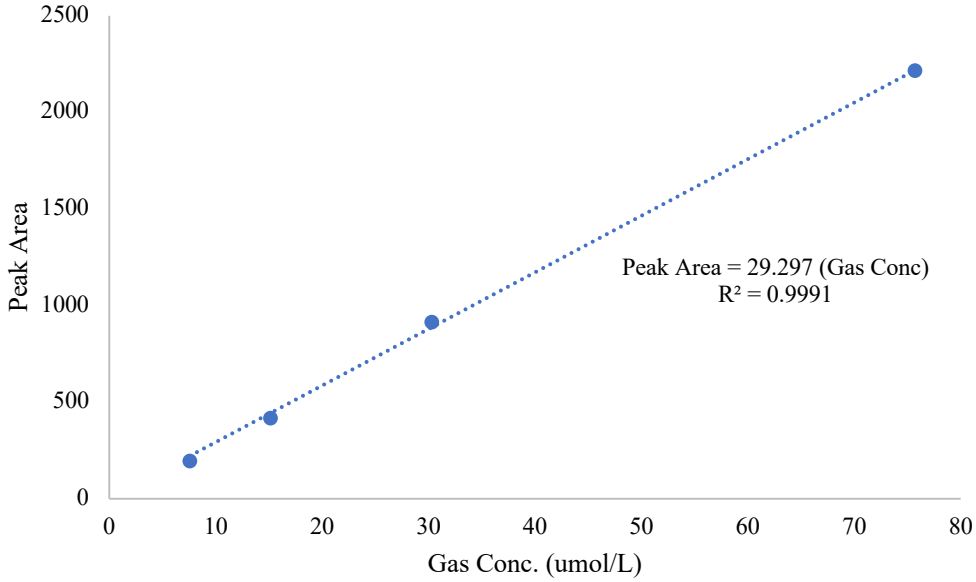

Figure 79: Standard curve for ethene on gas chromatograph. Dotted line represents linear relationship between peak area and concentration ethene in the gas phase. Data points represent an average of three trials. Error bars represent standard deviation between trials. Standard deviation small so error bars are barely visible.

Appendix B: Tables

Table 1: Henry's constants for chlorinated ethenes and ethene

Compound	**Abbreviation**	**Henry's Constant[41] (M/atm)**	**Converted Dimensionless Henry's Constant at 25°C (Cg/Cl)**
Vinyl Chloride	VC	3.80E-02	1.076
1,2-dichlorothene	cDCE	2.70E-01	0.151
Ethene	Ethene	4.70E-03	8.701
Trichloroethene	TCE	1.10E-01	0.372

Table 2: Anaerobic media solution

M1		M2		M3		M4		M5	
		Mineral solution per 1L of DI water		Trace metals solution per 1L of DI water		Vitamin stock solution per 1L DI water			
Chemical	Mass (g)	Chemical	Mass (g)	Chemical	Mass (g)	Chemical	Mass (g)	Chemical	Mass (mg)
K_2HPO_4	1	$NaCl$	2.27	$FeCl_2 \cdot 4H_2O$	1	biotin	0.002	Na_2S	15
Na_2CO_3	3	NH_4Cl	27.3	$MnCl_2 \cdot 4H_2O$	1	folic acid	0.002	Yeast extract	20
$Resazurin$	0.001	KCl	5	$CoCl_2 \cdot 6H_2O$	0.2	pyridoxine	0.01		
		KH_2PO_4	5	H_3BO_3	0.12	riboflavin	0.005		
		$MgCl_2 \cdot 6H_2O$	5	$ZnCl_2$	0.02	thiamin	0.005		
		$CaCl_2 \cdot 2H_2O$	2	$CuCl2 \cdot 2H_2O$	0.02	nicotinic acid	0.005		
				$NiCl_2 \cdot 6H_2O$	0.02	pantothenic acid	0.005		
				$Na_2MoO_4 \cdot 2H_2O$	0.02	B12	0.005		
				$Na_2WO_4 \cdot 2H_2O$	0.02	aminobenzoic acid	0.005		
				$Al_2(SO_4)_3 \cdot 18H_2O$	0.04	thioctic acid	0.005		
				HCl	10 mL of 1N				

Modification of ES&T 1998, vol. 32, no. 22, p. 3591-3597 (McCarty)

Table 3: List of materials for encapsulation

Material	**Quantity**	**Preparation**
Scoopula	2	(1)
Stir Bars	2	(1)
500 mL Glass Beakers	2	(1)
Plastic Filter Funnel	1	(1)
158 mL Borosilicate Wheaton bottles	6	(1)
20 mL plastic syringe	2	(2)
23 G Needle	2	(2)
16G Needle	2	(2)
500 mL Nitrogen Purged Waste Bottle	1	(1)
pH strips	--	--
0.25% $CaCl_2$	800 mL	(3)

Material	Quantity	Preparation
Anaerobic Media*	800 mL	(3)
15,000 ppm NaS_2	1mL	--
Solution 2**	1 mL	--
Chemicals		
Name	**Brand**	**Purity (%)**
Resazurin	Aldrich Chemical Company	98
Alginate	Spectrum Chemical MFG Corp.	99
Trichlorethylene	Alt Aesar	99.9
1,2-dichloroethylene	Alfa Aesar	99
Vinyl Chloride	Aldrich Chemical Company	99.5
Ethene	Airgas	--

* Media solution adapted from Yang and McCarty (1998)[33] (See Table 2).

**See Table 4

(1) Materials autoclaved and wrapped in tinfoil with vent holes and placed in anaerobic glove box 48-72 hours in advance of experiment.

(2) Sterile plastic syringes were opened in the anaerobic glove box and filled with chamber gas 3 times before being left filled for 48-72 hours in advanced of experiment due to oxygen trapped in plastic pores. Needles packages were opened for the same reason.

(3) Solution made anaerobic before entering glove box.

Table 4: Solution 2 constituents

Chemical	Mass (g)
K_2HPO_4	155
NaH_2PO_4	85
Ultra-pure water	1000 (mL)

Appendix C: Equations

Nomenclature

Symbol	Variable	Units
M_t	Mass total	mg
V_g	Volume of gas compartment	L
V_l	Volume of liquid compartment	L
C_g	Concentration in the gas phase	mg/L
C_l	Concentration in the liquid phase	mg/L
H_{cc}	Dimensionless Henry's Constant (Cg/Cl)	--
H_{pi}	Henry's Constant	M/atm
R	Ideal gas constant	L·atm/mol·K
n_{TCE}	Moles TCE	mol
n_{cDCE}	Moles cDCE	mol
n_{VC}	Moles VC	mol
n_{Ethene}	Moles Ethene	mol

Symbol	Variable	Units
P	Pressure	atm
V	Volume	L
T	Temperature	K
C_1	Oxygen concentration of atmospheric air	%
C_2	Oxygen concentration in headspace of reactor	%
V_1	Volume of air added	mL
V_2	Headspace of reactor	mL

Equations

(1) Total Mass of a CAH

$$M_t = V_g C_g + V_l C_l$$

(2) Henry's Law

$$H_{cc} = C_g / C_l$$

(3) Converted Linear Rate Mole Totals

$$n_{TCE} = n_{cDCE} + n_{VC} + n_{Ethene}$$

$$n_{cDCE} = n_{VC} + n_{Ethene}$$

$$n_{vc} = n_{Ethene}$$

(4) Creating a 0.97% Oxygen headspace

$$C_1 V_1 = C_2 V_2$$
$$C_2 = \frac{C_1 V_1}{V_2}$$
$$C_2 = \frac{(0.21)(5\ mL)}{(108\ mL)} = 0.0097 \rightarrow 0.97\%$$

(5) Estimating cell mass per bead

$$\frac{0.46\ mg\ cells}{20\ mL\ gel} = 0.023 \frac{mg\ cells}{mL\ gel}$$
$$Volume\ of\ Bead = \frac{4}{3}\pi r^2$$
$$Assume\ uniform\ bead\ diameter, D_{bead} \cong 3\ mm$$
$$Volume\ of\ Bead = \frac{4}{3}\pi(1.5mm)^2 = 14.14\ mm^3 = 0.01414\ cm^3 = 0.014\ mL$$

$$Mass\ cells\ per\ bead = \frac{0.01414\ mL}{bead}\left(0.023\ mg\frac{cells}{mL}\right) = 3.25\ \times 10^{-4}\ \frac{mg\ cell}{bead}$$

(6) Estimating cell growth after one addition TCE

$Protien\ produced\ per\ dechlorination = \frac{0.006\ mg\ Protien}{umnol\ Cl^{-}dechlorinated}$ (Estimation from a similar dechlorinating culture [42]

$Moles\ chlorine\ dechlorinated\ 2.5\ umol\ TCE * 3\ Cl^{-} = 7.5\ umol\ Cl^{-}$

$\frac{0.006\ mg\ Protien}{umol\ Cl^{-}dechlorinated}(7.5\ umol\ Cl^{-1})\left(\frac{2\ mg\ TSS}{mg\ protien}\right) = 0.09\ mg\ TSS\ generated\ per\ spike\ TCE$